Journal of Medicinal Chemistry

Article

Design and Synthesis of Novel Amino-triazine Analogs as Selective Bruton's Tyrosine Kinase Inhibitors for Treatment of Rheumatoid Arthritis

Wataru Kawahata, Tokiko Asami, Takao Kiyoi, Takayuki Irie, Haruka Taniguchi, Yuko Asamitsu, Tomoko Inoue, Takahiro Miyake, and Masaaki Sawa

J. Med. Chem., **Just Accepted Manuscript** • Publication Date (Web): 14 Sep 2018

ACS Publications

is published by the American Chemical Society. 1155 Sixteenth Street N.W., Washington, DC 20036

Design and Synthesis of Novel Amino-triazine Analogs as Selective Bruton's Tyrosine Kinase Inhibitors for Treatment of Rheumatoid Arthritis

Wataru Kawahata, Tokiko Asami, Takao Kiyoi, Takayuki Irie, Haruka Taniguchi, Yuko Asamitsu, Tomoko Inoue, Takahiro Miyake and Masaaki Sawa*

Research and Development, Carna Biosciences, Inc., 3rd Floor, BMA, 1-5-5 Minatojima-Minamimachi, Chuo-ku, Kobe 650-0047, Japan

KEYWORDS. Kinase inhibitor, Bruton's tyrosine kinase, BTK, CIA model, Rheumatoid arthritis, Amino-triazine.

ABSTRACT

Bruton's tyrosine kinase (BTK) is a promising drug target for the treatment of multiple diseases such as B cell malignances, asthma, and rheumatoid arthritis. A series of novel aminotriazines were identified as highly selective inhibitors of BTK by a scaffold hopping approach. Subsequent SAR studies of this series using two conformationally different BTK proteins, an activated form of BTK and an unactivated form of BTK, led to the discovery of a highly

selective BTK inhibitor **4b**. With significant efficacies *in vivo* models and a good ADME and safety profile, **4b** was advanced into preclinical studies.

INTRODUCTION

Bruton's tyrosine kinase (BTK) is a member of the Tec family of non-receptor tyrosine kinases, and expressed mainly in all hematopoietic cells, especially in B-cells and myeloid cells, but very low expression level of BTK is found in T-cells, natural killer cells and plasma cells.[1-3] BTK is essential for B-cell maturation by mediating the B-cell receptor (BCR) signaling, and also plays a crucial role in macrophages and mast cell activation via the high-affinity IgE receptor (FcεRI) to release several pro-inflammatory mediators.[4-7] The implication of BTK in a number of pathological processes has been reported, and thus BTK has emerged as a promising target for new therapeutic interventions in a wide array of diseases involving B-cell and/or macrophage activation, such as B-cell malignancies, asthma, rheumatoid arthritis and systemic lupus erythematosus.[8-10] Ibrutinib, the first FDA-approved covalent BTK inhibitor, has demonstrated impressive response rates in patients with mantle cell lymphoma and chronic lymphocytic leukemia,[11] and several second generation covalent BTK inhibitors are currently being evaluated in clinical trials for treating those B-cell malignancies.[12] These BTK inhibitors covalently bind to Cys481 residue in the ATP binding site of BTK to inhibit BTK enzymatic activity irreversibly. However, there is still a high demand for non-covalent BTK inhibitors for the treatment of autoimmune diseases because of the propensity of Michael acceptors to form reactive metabolites.[13] In addition, the use of kinase inhibitors for non-oncology indications is thought to be a difficult challenge due to anticipated adverse effects related to off-target activities

of inhibitors.[14-16] Hence, it is significantly important to optimize kinase selectivity for producing safer drugs, and a number of selective non-covalent BTK inhibitors are also under evaluation in a clinical trials.[17] As a part of our effort to develop selective and non-covalent BTK inhibitors, we previously reported a series of novel pyrimidine analogs as highly selective and reversible inhibitors of BTK represented by an initial lead compound **1**.[18] Unfortunately, efforts to optimize the compound **1** were unsuccessful due to the hERG inhibitory activities of this chemical series, which would cause QT prolongation. In this article, we describe the design and synthesis of novel and potent triazine-based inhibitors for BTK to overcome the hERG issue by a scaffold hopping approach from compound **1**.

RESULTS AND DISCUSSION

In the course of our work on the pyrimidine-based analogs, those compounds were found to show hERG inhibitions, which seemed difficult to eliminate by modifying substituents. Therefore, we turned our attention to exploration of a new scaffold. Namely, we got interested in replacing the pyrimidine core with a N-containing heteroaryl group, in which the nitrogen atom would act as the H-bond acceptor to interact with the hinge region of BTK (Figure 1).

Firstly, we synthesized heteroaryl analogs **2a**-**2c** by replacing the pyrimidine ring of compound **1** with other possible N-containing heteroaryl rings, and tested for the inhibition of two conformationally different recombinant human BTK enzymes, an activated conformation of BTK (BTK[A]) and an unactivated conformation of BTK (BTK[U]), based on the fact that compounds preferentially binding to BTK[U] would show higher kinase selectivity than compounds bind to BTK[A] as we previously reported.[19, 20]

It can be seen from the results in Table 1, all compounds synthesized here exhibited more potent inhibition for BTK[U] as expected, because the parent compound **1** was designed to bind BTK[U] preferentially. The pyrazine (**2a**), 1,3,4-triazine (**2b**) and 1,3,5-triazine (**2c**) showed weak inhibition for BTK[A] with IC_{50} values in the micromolar range (1.8 -5.6 μM). The 1,3,4-triazine (**2b**) and 1,3,5-triazine (**2c**) displayed strong inhibition for BTK[U] (IC_{50} = 10 and 6.4 nM, respectively), but the pyrazine (**2a**) was less potent for BTK[U] (IC_{50} = 100 nM). These results suggested that the nitrogen atom at 3-position of the central heteroaryl ring was important for the inhibitory potency for BTK[U]. In our previous paper, the docking model of the pyrimidine analog with BTK suggested that the 4-position of the pyrimidine ring seem to be able to interact with the hinge region of BTK.[18] Therefore, we next examined the effects of substituents at the 4-position of the 1,3,5-triazine ring. Introduction of methyl group resulted in a decrease of inhibitory potency (**2d**, IC_{50} = 7800 and 37 nM for BTK[A] and [U], respectively). Incorporation of amino group into compound **2c** to give compound **2e**, which displayed a dramatic improvement of inhibitory potency for both BTK[A] and [U] with IC_{50} values of 190 and 0.67 nM, respectively. The methoxy analog **2f** was significantly less potent for BTK[U] (IC_{50} = 80 nM), and the demethylation (**2g**) led to further decrease of the inhibitory potency even though it has a hydrogen bond donor similar to the amino analog (IC_{50} = 8800 nM for BTK[U]).

To probe the binding mode of the 1,3,5-triazine analog, we determined the X-ray co-crystal structure of **2e** complexed with BTK. As shown in Figure 2, **2e** binds in the ATP binding pocket of BTK adopting a Src-like inactive conformation which has been reported previously.[21] The *t*-butylphenyl group of compound **2e** occupies a back pocket, so-called the H3 pocket. Compound **2e** also forms several important hydrogen bonds with the hinge region of BTK. The NH at 2-position and the nitrogen atom at 3-position of the central triazine ring make two hydrogen bonds

with the backbone carbonyl and NH of Met477, respectively. The NH_2 at 4-position of the triazine ring is engaged in an extra H-bond interaction with the backbone carbonyl of Glu475. The benzene ring at 6-position of the triazine makes a favorable hydrophobic interaction with Val416, and the methyl substituent on the benzene further enhances this hydrophobic interaction. The X-ray co-crystal structure of **2e** bound to BTK revealed that more space is available around this methyl group, where Asp539 and Lys430 can provide additional interactions with the compound. Thus, we synthesized **2h** by introducing a hydroxyl group at the methylbenzene which is capable of making H-bonds. As expected, this modification further improved the inhibitory potency for both BTK[A] and BTK[U] (Table 1, IC_{50} = 43 and <0.3 nM for BTK[A] and [U], respectively). Based on those results, we selected **2h** having the 1,3,5-triazine ring for further optimization.

The previous work in our laboratory has demonstrated that in the right-hand side (RHS) part, the benzoylmorpholine moiety can be replaced with the 4-morpholinophenyl, which would result in better *in vitro* ADME property.[18] In fact, 4-morpholinophenyl analog **3a** showed a 2-fold increase in Caco-2 cell permeability compared with the benzoylmorpholine analog **2h** ($P_{app}\times10^6$/cm·s^{-1} = 7.4 and 16.3 for **2h** and **3a**, respectively) while the kinase inhibitory potency against BTK of **3a** was comparable to the that of **2h** (Table 2). Thus, we initiated our efforts to explore the SAR on the left-hand side (LHS) which would interact with the H3 hydrophobic pocket of BTK while keeping the central aminotriazine ring unchanged and the RHS constant as 4-morpholinophenyl. Realizing the metabolic lability of the terminal *t*-butyl group in **3a** as we previously described,[18] we focused our efforts on exploring replacement of the *t*-butyl group to improve the metabolic stability. Replacement with isopropyl (**3b)** or cyclopropyl (**3c)** resulted in a slight decrease of potency for both BTK[A] and [U], although cyclopropyl analog **3c** showed

improved metabolic stability in human liver microsomes. Introduction of dimethylamino group (**3d)** led to further improvement in microsomal stability in both human and mouse while the inhibitory potency for BTK[A] was maintained. However, 6-fold decrease of inhibitory potency for BTK[U] was observed, suggesting the H3 pocket in BTK[A] and BTK[U] have different sensitivity to substituents at the terminal benzene. Replacement of the benzene ring with thiazole (**3e**) or thiophene (**3f)** resulted in a significant decrease of potency for BTK[A], while the decrease of the potency for BTK[U] was modest. Compound **3g** having tetrahydrobenzothiophene was equipotent to compound **3a**, but this substitution did not improve the metabolic stability.

Up to this point, all compound synthesized showed poor metabolic stability, presumably due to the lability of the amide bond linking the terminal benzene in addition to the *t*-butyl group metabolism that reported previously.[22] In an attempt to improve the metabolic lability by modifying the terminal benzene on the LHS, we next designed various cyclic amide analogs (Table 3). Cyclization of **3a** or **3c** led to deterioration of the potency for both BTK[A] and [U] (compounds **3h**-**j**), but this cyclization resulted in a significant improvement of the metabolic stabilities in both human and mice liver microsomes (compound **3i**). Introduction of fluorine atom and cyano group into the terminal *t*-butyl benzene (**3k**) improved the potency while maintaining the metabolic stability. Replacing of cyanopropane group in **3k** with cyclopropyl group (**3l**) further improved BTK inhibitory potency (70 nM for BTK[A]), but showed poor stability in mouse liver microsomes. Incorporation of double bond into the cyclic amide (**3m)** resulted in a remarkable improvement of BTK inhibition (vs **3l**, 4.1-fold and 5.3-fold for BTK[A] and BTK[U], respectively), but with moderate metabolic stability. Compound **3n** having dihydropyrrolopyrazine retained potency, but not sufficient to switch due to the metabolic

instability. Thus, it was concluded that the dihydroisoquinolone core with cyclopropyl group and fluorine atom was optimal for potency with acceptable metabolic stability as with the case of our previous report.[18]

Exploration of the SAR on the RHS was conducted to optimize the potency and physicochemical property. Based on the SAR results on the pyrimidine-based inhibitors described in the previous study,[18] we focused our efforts on exploring substitution on the pyrazole and pyrrole ring. Thus, a small set of N-substituted pyrazole and pyrrole analogs was synthesized to evaluate the potency and physicochemical property (Table 4). Replacement of the morpholinobenzene with pyrazole as in compound **4a** resulted in approximately 2-fold improvement of the inhibitory potency for BTK[A] with substantial metabolic stabilities and aqueous solubility compared with **3m**. The methyl substitution on the pyrazole (**4b**) led to a further improvement of the potency for both BTK[A] and BTK[U] while maintaining good metabolic stabilities and aqueous solubility. Further substitution of the pyrazole ring with bulky aliphatic groups, such as cyclopropyl (**4c)** or cyclopropylethyl (**4d)** sustained BTK inhibitory potency but the metabolic stabilities and aqueous solubilities were reduced. Substituted cyanopyrrole (**4e**-**4i**) exhibited similar inhibitory potencies but did not show the improvement in metabolic stabilities and aqueous solubilities.

Compound **4b** and **4e** having *N*-methyl-pyrazole and *N*-methyl-cyanopyrrole, respectively, were screened over a panel of 312 kinases to evaluate the kinase selectivity (Table S1). Both of compounds demonstrated an excellent kinase selectivity with a similar profile, only two Tec family kinases were inhibited at 0.3 μM concentration (BMX, 80% and 84.3% inhibitions for **4b** and **4e**, respectively; TEC, 99.5% and 99.2% inhibitions for **4b** and **4e**, respectively). TEC and BMX have been reported to be implicated in inflammation,[6] this selectivity profile might be

beneficial for the treatment of RA. On the other hand, ibrutinib was found to be inhibit both BTK[A] and BTK[U] strongly (0.54 and 0.33 nM, respectively). Ibrutinib showed a moderate selectivity profile (34 kinases inhibited more than 50% at 0.3 μM), supporting our strategy to obtain selective BTK inhibitors by increasing BTK[A]/BTK[U] ratio.

As described previously, the pyrimidine-based analogs showed hERG inhibition. Therefore, safety profiling of those compounds was conducted against hERG channel (Table 4). All triazine analogs tested showed moderate to no effects on hERG. Importantly, **4b**, **4g** and **4h** showed greatly reduced activities in the hERG assay. Methylpyrazole analog **4b** showed an improved hERG inhibition (IC_{50} = 24 μM) compared with the corresponding pyrimidine-based analogs (IC_{50} = 14 μM).[18] Methylpyrazole analog **4b** met all of our *in vitro* assay criteria, and thus selected for the further evaluations.

We next evaluated the cellular potency of **4b** by measuring anti-IgM-stimulated phosphorylation of BTK and PLCγ2 in Ramos cells. Upon BCR activation by anti-IgM treatment, Tyr551 is phosphorylated by upper signal kinases, such as LYN and SYK, followed by autophosphorylation of Tyr223 to activate BTK, then the activated BTK phosphorylates PLCγ2 that induces intracellular calcium mobilization. As shown in Figure 3, compound **4b** potently inhibited those phosphorylations with an IC_{50} values of 19, 14 and 26 nM, respectively. Furthermore, **4b** significantly inhibited anti-IgM induced B cell activation (CD86 expression) in human PBMC with IC_{50} value of 13 nM.

With the strong cellular potency and excellent kinase selectivity profile, compound **4b** was further evaluated *in vivo*. In pharmacokinetics (PK) studies of **4b** using multiple species, **4b** exhibited good PK profiles with the oral bioavailabilities of 65 % in mice, 44 % in rats, and 43 % in dogs (Table 5). Based on its adequate exposure in animals, **4b** was advanced into several

mouse models of inflammatory and autoimmune diseases to examine its *in vivo* efficacy. For those animal models, we have used the following vehicle; DMSO:PEG#400:HP-β-CD [30%(w/v)] (5:30:65), to solubilize **4b**.

Firstly, we examined the effects of **4b** on FcεRI-mediated type I allergy in a passive cutaneous anaphylaxis (PCA) mouse model to evaluate the anti-inflammatory efficacy.[23] Oral administration of **4b** at 30 mg/kg significantly inhibited the PCA reaction, and its inhibition rate was 69% as compared to vehicle control (Figure 4).

Next, we tested **4b** in collagen-induced arthritis (CIA) mouse model to investigate the efficacy on autoimmune disease. [23] Compound **4b** was administered orally (15, 30 and 60 mg/kg, b.i.d.) for 19 days, and inhibition of arthritis development was evaluated by measuring clinical arthritis index (AI), which reflecting paw swelling and joint inflammation. As shown in Figure 5, a marked reduction in severity of AI was observed in dose-dependent manner, suggesting compound **4b** attenuates arthritis development by inhibiting BTK *in vivo*.

Syntheses of pyrazine **2a** and 1,3,5-triazine analogs **2b**-**2h** are shown in Scheme 1. Commercially available 3-amino-2-methylphenylboronic acid pinacol ester **5** was coupled with 4-*t*-butylbenzoyl chloride to give boronate ester **6**. (4-Amino-phenyl)(morpholino)methanone **7** was coupled with 2,6-dichloropyrazine by Buchwald-Hartwig reaction, and then the resulting chloropyrazine **8** was coupled with boronate ester **6** by Suzuki-Miyaura cross-coupling reaction to give pyrazine **2a**. 1,3,5-Triazine analogs **2c**-**2g** were obtained in a manner similar to the synthesis of **2a** using the appropriate dichloro-1,3,5-triazines. Demethylation of **2f** afforded the corresponding hydroxy triazine derivative **2g**.

1,2,4-Triazine **15** was synthesized from commercially available methyl 2-amino-benzoate **10**. Namely, coupling of **10** with 4-*t*-butylbenzoyl chloride, followed by hydrolysis of the methyl

ester gave carboxylic acid **12**. The carboxyl group in **12** was then converted to acetyl group using methylmagnesium bromide via Weinreb amide **13**. The resulting acetophenone **14** was oxidized by selenium oxide, followed by cyclization with *S*-methylisothiosemicarbazide furnished 1,2,4-triazine **15**.[24] Finally, desulfurative cross-coupling reaction[25] of **15** with aniline **7** gave the desired 1,2,4-triazine **2b**.

The hydroxymethyl benzene analog **2h** was synthesized from commercially available (2-bromo-6-nitrophenyl)methanol **16**. Protection of the hydroxyl group in **16** with TBS group, followed by reduction of the nitro group of **17** afforded aniline **18**, which was then subjected to amide coupling with 4-*t*-butylbenzoyl chloride to give **19**. The bromo group in **19** was converted to a boronate ester group by treating with bis(pinacolato)diboron. The resulting boronate ester **20** was then coupled with **9e** by Suzuki−Miyaura cross-coupling, followed by TBAF treatment yielded the desired compound **2h**.

The general procedure for the preparation of 1,3,5-triazine derivatives with various R^2 groups listed in Table 2 and 3 is shown in Scheme 2, through Suzuki-Miyaura cross-coupling of the key chloro-triazine intermediate **22**. 2-Amino-4,6-dichloro-1,3,5-triazine was treated with 4-morpholinoaniline to give common intermediate **22**. The required boronate esters **23b-g**, **24h-m** and **25** were prepared analogously according to the method reported literature (see supporting information). Diamino chlorotriazine **22** was coupled with appropriate boronate esters **20**, **23b-g**, **24h-m** and **25** by Suzuki-Miyaura cross-coupling, followed by deprotection of the hydroxyl group furnished the desired 1,3,5-triazine derivatives. In some cases (**3h**, **3j**, and **3n**), the removal of the acetyl group was observed during the coupling reaction.

The five-membered heterocyclic aminotriazine analogs **4a-4i** were synthesized in 2 steps starting from common intermediate **24m** as shown in Scheme 3. The pyrazole derivatives **26a-**

26d and pyrrole derivative **26e-26i** were readily prepared from 2-amino-4,6-dichloro-1,3,5-triazine and appropriately substituted aminopyrazoles or aminopyrroles as previously described.[18] The coupling conditions of **24m** and chlorotriazines **26a-26i** were identical to the one described above. Acetyl group was successfully removed by transesterification as described in Scheme 2. For **4a**, THP group was deprotected by treating with TsOH before transesterification.

CONCLUSION

Scaffold hopping strategy to eliminate the hERG inhibition was successfully applied to the identification of novel aminotriazine derivatives as potent inhibitors of BTK. The detailed SAR studies using two conformationally different recombinant human BTK enzymes, an activated conformation of BTK and an unactivated conformation of BTK, led to the discovery of **4b** with a significant kinase selectivity profile. Compound **4b** exhibited the strong inhibitory potency for the BCR activation in B-cells and showed excellent PK profiles in multiple species. In a mouse CIA model, **4b** significantly reduced paw swelling and joint inflammation in a dose-dependent manner. Based on the *in vitro* potencies, PK profiles and *in vivo* efficacies, compound **4b** was advanced into preclinical development studies.

EXPERIMENTAL SECTION

General Procedures. Reagents and solvents were purchased from commercial sources and used without further purification. All reactions involving air- or moisture-sensitive reagents were performed under a nitrogen atmosphere unless otherwise noted. Microwave reactions were run in

a Biotage Initiator set to normal power at the indicated temperature and were performed in sealed microwave reaction vessels. Thin layer chromatography (TLC) was carried out using Merck GmbH Precoated silica gel 60 F254 plates. Silica gel chromatography refers to the use of an automated medium pressure flash chromatography system (Teledyne ISCO or Yamazen Corp.) using prepacked silica gel cartridges with UV detection at 254 nm. Preparative reverse-phase HPLC (prep-HPLC) was performed on a Waters Autopurification system (dual triggered by target mass and UV 254 nm) using Imtakt Unison US-C18, 5 mm, 50 mm × 20 mm I.D. column, eluting with a binary solvent system A and B using a gradient elution (A, 10 mM formic acid aq.; B, 10 mM formic acid in MeOH). All yields reported are isolated yield after removal of residual solvents. The purity of a purified compound was determined using Shimazu Prominence HPLC system by UV detection (215 nm) with collecting MS spectra (100-800 *m/z* scan) of the target peak. The separation method is shown as following. Column: Imtakt Cadenza, 3 mm, 50 mm × 2.0 mm I.D. Mobile phase: acetonitrile in water (10 mM formic acid) from 10% to 90% with total 5 min run. Flow rate: 0.5 mL/min. ^{1}H -NMR spectra were recorded on Burker Ultra Shield™ 400 Plus; chemical shifts (δ) are reported relative to a signal of TMS. Data format of NMR spectra is as follows: chemical shift (δ ppm), multiplicity (s = singlet, br = broad signal, d = doublet, t = triplet, q = quartet, dd = doublet of doublets, dt = doublet of triplets, ddd = doublet of doublet of doublets, m = multiplet or overlapping), coupling constant (Hz), and integration. Very broad peaks for protons on hetero atoms are not always indicated. The synthesized compounds for biological assay have over 95% purity, otherwise noted in each synthesis experimental below.

4-(*t*-Butyl)-*N*-[2-methyl-3-(6-{[4-(morpholine-4-carbonyl)phenyl]amino}pyrazin-2-yl)phenyl]benzamide (2a). A mixture of **8** (53 mg, 0.17 mmol) and **6** (66 mg, 0.17 mmol) in

DME (3 mL) was degassed with N_2 for 5 min. To this mixture, $Pd(PPh_3)_4$ (19 mg, 0.017 mmol) was added and degassed with N_2 for 5 minutes, subsequently $NaHCO_3$ (28 mg, 0.34 mmol) in water (1 mL) was added and degassed with N_2 for 2 min. The mixture was heated in the microwave reactor at 110 °C for 20 min. The reaction mixture was extracted with ethyl acetate (2×40 mL). The combined organic layers were washed by water (5 mL), and concentrated. The residue was purified by flash column chromatography using 50% ethyl acetate in hexane as eluent to afford **2a** as off-white solids (65mg, 0.118mmol, 69%). ^{1}H NMR (400 MHz, DMSO-d_6) δ 9.94 (s, 1H), 9.88 (s, 1H), 8.28 (s, 1H), 8.10 (s, 1H), 8.00 – 7.92 (m, 2H), 7.85 – 7.76 (m, 2H), 7.60 – 7.52 (m, 2H), 7.53 – 7.43 (m, 1H), 7.42 – 7.34 (m, 4H), 3.62 – 3.55 (m, 4H), 3.55 – 3.43 (m, 4H), 2.26 (s, 3H), 1.33 (s, 9H). ^{13}C NMR (101 MHz, DMSO) δ 169.5, 165.8, 154.9, 151.4, 151.3, 142.6, 138.9, 137.8, 134.3, 133.7, 132.8, 132.2, 128.9, 128.2, 128.0, 128.0, 127.9, 126.3, 125.7, 117.8, 66.6, 35.1, 31.4, 15.8.; HRMS (ESI) *m/z* calculated for $C_{33}H_{36}N_5O_3$ $[M+H]^+$: 550.2818, found: 550.2810, Purity 100%.

4-(*t*-Butyl)-*N*-[2-methyl-3-(3-{[4-(morpholine-4-carbonyl)phenyl]amino}-1,2,4-triazin-5-yl)phenyl]benzamide (2b). To a suspension of **15** (40 mg, 0.10 mmol) in toluene (2 mL) was added **7** (25 mg, 0.12 mmol), Copper(I) 3-methylsalicylate (44 mg, 0.20 mmol), Cs_2CO_3 (73 mg, 0.22 mmol), $PdOAc_2$ (2.29 mg, 10.19 nmol) and Xantphos (12 mg, 0.02 mmol). The mixture was heated in the microwave reactor at 170 °C for 3 hr. The reaction mixture was filtered through a bed of celite to remove insoluble materials. After removal of the solvent, the residue was purified by prep-HPLC to afford **2b** as off-white solids (8 mg, 0.013 mmol, 13 %). ^{1}H NMR (400 MHz, DMSO-d_6) δ 10.47 (s, 1H), 10.03 (s, 1H), 9.09 (s, 1H), 7.96 (d, J = 8.02 Hz, 2H), 7.89 (d, J = 8.31 Hz, 2H), 7.64 – 7.36 (m, 7H), 3.61 (br, 4H), 3.51 (br, 4H), 2.33 (s, 3H), 1.33 (s, 9H). ^{13}C NMR (101 MHz, DMSO) δ 169.5, 165.9, 155.4, 155.0, 150.8, 143.0, 141.4, 136.0, 134.6, 133.4,

132.0, 130.7, 129.6, 129.2, 128.7, 128.0, 126.7, 125.7, 119.1, 66.6, 35.2, 31.4, 15.8.; HRMS (ESI) *m/z* calculated for $C_{32}H_{35}N_6O_3$ $[M+H]^+$: 551.2771, found: 551.2759, Purity 97%.

4-(*t*-Butyl)-*N*-[2-methyl-3-(4-{[4-(morpholine-4-carbonyl)phenyl]amino}-1,3,5-triazin-2-yl)phenyl]benzamide (2c). To a solution of **9c** (50.0 mg, 0.16 mmol) and **6** (62 mg, 0.16 mmol) in DME (3 mL), $Pd(PPh_3)_4$ (18 mg, 0.016 mmol) and K_2CO_3 (43 mg, 0.31 mmol) in water (1 mL) were added, and the mixture was heated in the microwave reactor at 110 °C for 20 min. The reaction mixture was extracted with ethyl acetate (2×40 mL), and the combined organic layers were washed with water (5 mL), dried over sodium sulfate, filtered and concentrated. The crude material was purified by flash chromatography on silica gel, eluted with hexane/ethyl acetate to afford **2c** as colorless solids (25 mg, 0.045 mmol, 29%). ^{1}H NMR (400 MHz, DMSO-d_6) δ 10.56 (s, 1H), 9.97 (s, 1H), 8.91 (s, 1H), 7.99 – 7.89 (m, 2H), 7.89 – 7.82 (m, 2H), 7.68 – 7.24 (m, 7H), 3.66 – 3.54 (m, 4H), 3.56 – 3.40 (m, 4H), 2.39 (s, 3H), 1.33 (s, 9H). ^{13}C NMR (101 MHz, DMSO) δ 173.8, 168.8, 166.2, 165.3, 163.2, 154.4, 139.9, 137.3, 133.1, 132.1, 131.9, 131.9, 131.5, 131.4, 131.3, 128.7, 128.6, 127.9, 127.4, 125.5, 125.1, 119.8, 66.0, 34.6, 30.8, 15.4.; HRMS (ESI) *m/z* calculated for $C_{32}H_{35}N_6O_3$ $[M+H]^+$: 551.2771, found: 551.2770, Purity 97%.

Compounds **2d**, **2e** and **2f** were synthesized from 4-(*t*-butyl)-*N*-[2-methyl-3-(4,4,5,5-tetramethyl-1,3,2-dioxaborolan-2-yl)phenyl]benzamide (**6**) and the appropriate chlorotriazines **9d**, **9e** and **9f**, respectively, using a procedure similar to the procedure for the synthesis of **2c**.

4-(*t*-Butyl)-*N*-[2-methyl-3-(4-methyl-6-{[4-(morpholine-4-carbonyl)phenyl]amino}-1,3,5-triazin-2-yl)phenyl]benzamide (2d). Colorless solids; 66% yield. ^{1}H NMR (400 MHz, DMSO-d_6) δ 10.47 (s, 1H), 9.96 (s, 1H), 7.95 (d, J = 8.45 Hz, 2H), 7.87 (d, J = 8.25 Hz, 2H), 7.67 – 7.33 (m, 7H), 3.60 (br, 4H), 3.50 (br, 4H), 2.52 (s, 3H), 2.37 (s, 3H), 1.33 (s, 9H). ^{13}C NMR (101 MHz, DMSO) δ 174.4, 169.4, 165.8, 164.1, 154.9, 140.8, 137.8, 133.8, 133.7, 132.5, 132.1,

131.9, 130.0, 129.2, 128.5, 128.0, 126.0, 125.7, 120.1, 66.6, 35.2, 31.4, 26.0, 15.9.; HRMS (ESI) *m/z* calculated for $C_{33}H_{37}N_6O_3$ $[M+H]^+$: 565.2927, found: 565.2936, Purity 98.4%.

***N*-[3-(4-Amino-6-{[4-(morpholine-4-carbonyl)phenyl]amino}-1,3,5-triazin-2-yl)-2-methylphenyl]-4-(t-butyl)benzamide (2e).** Colorless solids; 30.7% yield. ^{1}H NMR (400 MHz, DMSO-d_6) δ 9.95 (s, 1H), 9.84 (s, 1H), 8.01 – 7.89 (m, 4H), 7.59 – 7.49 (m, 3H), 7.46 – 7.25 (m, 6H), 3.60 (br, 4H), 3.51 (br, 4H), 2.37 (s, 3H), 1.33 (s, 9H). ^{13}C NMR (101 MHz, DMSO) δ 174.7, 169.6, 167.3, 165.8, 164.7, 154.9, 141.9, 139.7, 137.6, 133.2, 132.2, 128.9, 128.4, 128.4, 128.0, 127.5, 125.7, 125.6, 119.5, 66.6, 35.1, 31.4, 15.8.; HRMS (ESI) *m/z* calculated for $C_{32}H_{36}N_7O_3$ $[M+H]^+$: 566.2880, found: 566.2874, Purity 98.9%.

4-(*t*-Butyl)-*N*-[3-(4-methoxy-6-{[4-(morpholine-4-carbonyl)phenyl]amino}-1,3,5-triazin-2-yl)-2-methylphenyl]benzamide (2f). Colorless solids; 68% yield. ^{1}H NMR (400 MHz, DMSO-d_6) δ 10.48 (br, 1H), 9.96 (s, 1H), 8.00 – 7.90 (m, 2H), 7.92 – 7.80 (m, 2H), 7.67 (d, J = 7.95 Hz, 1H), 7.58 – 7.53 (m, 2H), 7.50 – 7.45 (m, 1H), 7.42 (d, J = 8.26 Hz, 2H), 7.37 (t, J = 7.77 Hz, 1H), 4.01 (s, 3H), 3.60 (br, 4H), 3.50 (br, 4H), 2.39 (s, 3H), 1.33 (s, 9H). ^{13}C NMR (101 MHz, DMSO) δ 169.4, 165.8, 154.9, 140.7, 138.4, 137.9, 134.0, 132.5, 132.1, 132.0, 131.9, 130.1, 129.2, 128.5, 128.2, 128.0, 126.0, 125.7, 120.2, 66.6, 55.1, 35.2, 31.4, 16.0.; HRMS (ESI) *m/z* calculated for $C_{33}H_{37}N_6O_4$ $[M+H]^+$: 581.2876, found: 581.2883, Purity 100%.

4-(*t*-Butyl)-*N*-[3-(4-hydroxy-6-{[4-(morpholine-4-carbonyl)phenyl]amino}-1,3,5-triazin-2-yl)-2-methylphenyl]benzamide (2g). To a solution of **2f** (50 mg, 0.086 mmol) in MeOH (1 mL) was added 4N HCl in 1,4-dioxane (1 mL), and the mixture was stirred at 50 °C for 4 hr. The reaction mixture was diluted with 1N NaOH (30 mL), and extracted with ethyl acetate (3×25 mL). The combined organic layers were washed successively with water (20 mL) and brine (30 mL), dried over sodium sulfate, and concentrated. The crude material was purified by flash

chromatography on silica gel, eluted with chloroform/MeOH to afford **2g** as colorless solids (7 mg, 0.012 mmol, 14%). ^{1}H NMR (400 MHz, DMSO-d_6) δ 12.34 (s, 1H), 10.32 (s, 1H), 10.00 (s, 1H), 8.03 – 7.81 (m, 3H), 7.61 – 7.48 (m, 3H), 7.47 – 7.31 (m, 4H), 3.60 (br, 4H), 3.50 (br, 5H), 2.29 (s, 3H), 1.33 (s, 9H). ^{13}C NMR (101 MHz, DMSO) δ 169.4, 166.7, 165.9, 163.8, 155.9, 155.0, 140.7, 137.8, 133.7, 132.9, 132.1, 130.3, 129.8, 128.4, 128.1, 127.0, 126.3, 125.7, 120.2, 66.6, 35.2, 31.4, 15.5.; HRMS (ESI) *m/z* calculated for $C_{32}H_{35}N_6O_4$ $[M+H]^+$: 567.2720, found: 567.2706, Purity 100%.

***N*-[3-(4-Amino-6-{[4-(morpholine-4-carbonyl)phenyl]amino}-1,3,5-triazin-2-yl)-2-(hydroxymethyl)phenyl]-4-(*t*-butyl)benzamide (2h)**. To a solution of **9e** (256 mg, 0.764 mmol) in DME (11 mL) was added **20** (400 mg, 0.764 mmol), $Pd(PPh_3)_4$ (88 mg, 0.076 mmol), K_2CO_3 (211 mg, 1.53 mmol) and water (3.8 mL), and the mixture was heated in the microwave reactor at 110 °C for 20 min. The reaction mixture was diluted with water (50 mL) and extracted with ethyl acetate (3×25 mL). The combined organic layers were washed successively with water (50 mL) and brine (50 mL), then the organic layers were dried over sodium sulfate, and concentrated. The crude material was purified by flash chromatography on silica gel, eluted with hexane/ethyl acetate to afford the corresponding TBS protected intermediate. The obtained intermediate was dissolved in THF (4.1 mL), then 1 M TBAF solution in THF (0.4 mL) was added to the solution. The mixture was stirred for 16hr at room temperature. The solvent was evaporated, and the residue was purified by flash chromatography on silica gel, eluted with hexane/ethyl acetate to afford **2h** as colorless solids (62 mg, 0.11 mmol, 52%). ^{1}H NMR (400 MHz, DMSO-d_6) δ 10.41 (s, 1H), 9.85 (s, 1H), 8.09 – 7.95 (m, 1H), 7.95 – 7.83 (m, 4H), 7.65 – 7.54 (m, 2H), 7.50 (dd, J = 1.44, 7.78 Hz, 1H), 7.42 (t, J = 7.85 Hz, 1H), 7.36 (d, J = 8.63 Hz, 2H), 7.29 (br, 2H), 5.67 (t, J = 5.57 Hz, 1H), 4.83 (d, J = 5.58 Hz, 2H), 3.60 (br, 4H), 3.50 (br,

4H), 1.33 (s, 9H). ^{13}C NMR (101 MHz, DMSO) δ 174.0, 169.5, 167.0, 165.3, 164.5, 155.2, 141.7, 139.1, 138.5, 132.3, 132.1, 129.1, 128.4, 127.7, 127.5, 126.4, 126.0, 125.3, 119.6, 66.6, 58.4, 35.2, 31.4.; HRMS (ESI) *m/z* calculated for $C_{32}H_{36}N_7O_4$ $[M+H]^+$: 582.2829, found: 582.2833, Purity 100%.

Compounds **3a**, **3b**, **3c**, **3d**, **3e**, **3f** and **3g** were synthesized from 6-chloro-*N*^{2}-(4-morpholinophenyl)-1,3,5-triazine-2,4-diamine (**22**) and the appropriate boronate esters using a procedure similar to the procedure for the synthesis of **2h**.

***N*-(3-{4-Amino-6-[(4-morpholinophenyl)amino]-1,3,5-triazin-2-yl}-2-(hydroxymethyl)phenyl)-4-(*t*-butyl)benzamide (3a)**. Off-white solids; 34% yield. ^{1}H NMR (400 MHz, DMSO-d_6) δ 10.41 (s, 1H), 9.42 (br, 1H), 7.99 (s, 1H), 7.92 (d, *J* = 8.12 Hz, 2H), 7.71 – 7.54 (m, 4H), 7.51 (d, *J* = 7.43 Hz, 1H), 7.42 (t, *J* = 7.82 Hz, 1H), 7.16 (br, 2H), 6.89 (d, *J* = 8.60 Hz, 2H), 5.72 (br, 1H), 4.91 – 4.74 (m, 2H), 3.86 – 3.61 (m, 4H), 3.19 – 2.90 (m, 4H), 1.33 (s, 9H). ^{13}C NMR (101 MHz, DMSO) δ 178.1, 173.6, 167.0, 165.3, 155.2, 147.2, 139.4, 138.5, 132.3, 131.7, 127.5, 126.5, 126.0, 125.4, 122.0, 120.7, 115.9, 110.0, 66.6, 58.4, 49.5, 35.2, 31.4.; HRMS (ESI) *m/z* calculated for $C_{31}H_{36}N_7O_3$ $[M+H]^+$: 554.2880, found: 554.2877, Purity 96%.

***N*-(3-{4-Amino-6-[(4-morpholinophenyl)amino]-1,3,5-triazin-2-yl}-2-(hydroxymethyl)phenyl)-4-isopropylbenzamide (3b)**. Colorless solids; 15% yield. ^{1}H NMR (400 MHz, DMSO-d_6) δ 10.40 (s, 1H), 9.40 (br, 1H), 8.04 – 7.92 (m, 1H), 7.90 (d, *J* = 7.92 Hz, 2H), 7.71 – 7.54 (m, 2H), 7.52 – 7.34 (m, 4H), 7.17 (br, 2H), 6.88 (d, *J* = 8.53 Hz, 2H), 5.73 (br, 1H), 4.91 – 4.67 (m, 2H), 3.85 – 3.59 (m, 4H), 3.12 – 2.87 (m, 5H), 1.25 (d, *J* = 6.94 Hz, 6H). ^{13}C NMR (101 MHz, DMSO) δ 173.6, 167.0, 165.3, 164.4, 153.0, 147.2, 139.4, 138.4, 132.7,

132.3, 127.8, 127.6, 127.1, 126.5, 125.4, 122.0, 119.9, 115.9, 66.6, 58.4, 49.5, 33.9, 24.1.; HRMS (ESI) *m/z* calculated for $C_{30}H_{34}N_7O_3$ $[M+H]^+$: 540.2723, found: 540.2721, Purity 100%.

***N*-(3-{4-Amino-6-[(4-morpholinophenyl)amino]-1,3,5-triazin-2-yl}-2-(hydroxymethyl)phenyl)-4-cyclopropylbenzamide (3c)**. Off-white solids; 23% yield. ^{1}H NMR (400 MHz, DMSO-d_6) δ 10.36 (s, 1H), 9.41 (br, 1H), 8.04 – 7.90 (m, 1H), 7.90 – 7.77 (m, 2H), 7.60 (br, 2H), 7.49 (dd, *J* = 1.44, 7.80 Hz, 1H), 7.40 (t, *J* = 7.85 Hz, 1H), 7.28 – 7.21 (m, 2H), 7.15 (br, 2H), 6.95 – 6.80 (m, 2H), 5.68 (t, *J* = 5.72 Hz, 1H), 4.78 (d, *J* = 4.94 Hz, 2H), 3.85 – 3.63 (m, 4H), 3.15 – 2.92 (m, 4H), 2.11 – 1.94 (m, 1H), 1.11 – 0.96 (m, 2H), 0.82 – 0.72 (m, 2H). ^{13}C NMR (101 MHz, DMSO) δ 173.8, 173.6, 167.0, 165.2, 164.3, 148.8, 147.2, 139.4, 138.4, 132.2, 131.9, 127.7, 127.6, 126.5, 125.9, 125.4, 122.0, 115.9, 66.6, 58.4, 49.5, 15.7, 10.7.; HRMS (ESI) *m/z* calculated for $C_{30}H_{32}N_7O_3$ $[M+H]^+$: 538.2567, found: 538.2559, Purity 100%.

***N*-(3-{4-Amino-6-[(4-morpholinophenyl)amino]-1,3,5-triazin-2-yl}-2-(hydroxymethyl)phenyl)-4-(dimethylamino)benzamide (3d)**. Colorless solids; 31% yield. ^{1}H NMR (400 MHz, DMSO-d_6) δ 10.18 (s, 1H), 9.40 (br, 1H), 8.02 (d, *J* = 7.80 Hz, 1H), 7.88 – 7.75 (m, 2H), 7.61 (br, 2H), 7.48 – 7.31 (m, 2H), 7.14 (br, 2H), 6.94 – 6.84 (m, 2H), 6.84 – 6.74 (m, 2H), 5.87 – 5.59 (m, 1H), 4.93 – 4.70 (m, 2H), 3.79 – 3.65 (m, 4H), 3.06 – 3.02 (m, 4H), 3.01 (s, 6H). ^{13}C NMR (101 MHz, DMSO) δ 173.7, 167.0, 165.2, 164.3, 153.0, 147.2, 139.3, 139.0, 132.3, 129.0, 127.5, 125.7, 124.8, 121.9, 121.2, 115.9, 115.1, 111.5, 66.6, 58.5, 49.5.; HRMS (ESI) *m/z* calculated for $C_{29}H_{33}N_8O_3$ $[M+H]^+$: 541.2676, found: 541.2668, Purity 100%.

***N*-(3-{4-Amino-6-[(4-morpholinophenyl)amino]-1,3,5-triazin-2-yl}-2-(hydroxymethyl)phenyl)-5-(*t*-butyl)thiazole-2-carboxamide (3e).** Off-white solids; 14% yield. ^{1}H NMR (400 MHz, DMSO-d_6) δ 10.44 (s, 1H), 9.45 (br, 1H), 8.39 (s, 1H), 7.70 (d, *J* = 8.07 Hz,

1H), 7.66 – 7.47 (m, 3H), 7.41 (t, *J* = 7.85 Hz, 1H), 7.19 (br, 2H), 6.99 – 6.78 (m, 2H), 5.50 (br, 1H), 4.70 (s, 2H), 3.81 – 3.65 (m, 4H), 3.13 – 2.94 (m, 4H), 1.42 (s, 9H).

^{13}C NMR (101 MHz, DMSO) δ 190.3, 185.3, 173.4, 166.8, 164.3, 159.5, 151.1, 147.3, 143.8, 139.6, 137.1, 134.4, 132.1, 127.8, 127.2, 122.1, 115.9, 66.6, 57.9, 49.5, 38.3, 30.8.; HRMS (ESI) *m/z* calculated for $C_{28}H_{33}N_8O_3S$ $[M+H]^+$: 561.2396, found: 561.2390, Purity 100%.

***N*-(3-{4-Amino-6-[(4-morpholinophenyl)amino]-1,3,5-triazin-2-yl}-2-(hydroxymethyl)phenyl)-5-(*t*-butyl)thiophene-2-carboxamide (3f)**. Colorless solids; 44% yield. ^{1}H NMR (400 MHz, DMSO-d_6) δ 10.31 (s, 1H), 9.42 (br, 1H), 7.81 (d, *J* = 7.91 Hz, 1H), 7.68 (d, *J* = 3.84 Hz, 1H), 7.60 (br, 2H), 7.51 (dd, *J* = 1.40, 7.78 Hz, 1H), 7.39 (t, *J* = 7.85 Hz, 1H), 7.17 (br, 2H), 7.03 (d, *J* = 3.84 Hz, 1H), 6.93 – 6.84 (m, 2H), 5.63 (t, *J* = 5.85 Hz, 1H), 4.74 (d, *J* = 6.20 Hz, 2H), 3.80 – 3.63 (m, 4H), 3.12 – 2.94 (m, 4H), 1.38 (s, 9H). ^{13}C NMR (101 MHz, DMSO) δ 173.6, 166.9, 164.3, 163.2, 160.4, 147.2, 139.5, 137.8, 136.6, 132.2, 129.0, 127.7, 126.9, 126.1, 123.5, 122.0, 115.9, 66.6, 58.2, 49.5, 40.6, 35.1, 32.4.; HRMS (ESI) *m/z* calculated for $C_{29}H_{34}N_7O_3S$ $[M+H]^+$: 560.2444, found: 560.2455, Purity 100%.

***N*-(3-{4-Amino-6-[(4-morpholinophenyl)amino]-1,3,5-triazin-2-yl}-2-(hydroxymethyl)phenyl)-4,5,6,7-tetrahydrobenzo[b]thiophene-2-carboxamide (3g)**. Pale-yellow solids; 24% yield. ^{1}H NMR (400 MHz, DMSO-d_6) δ 10.30 (s, 1H), 9.43 (br, 1H), 7.88 (s, 1H), 7.68 – 7.57 (m, 2H), 7.57 – 7.45 (m, 2H), 7.40 (t, *J* = 7.83 Hz, 1H), 7.17 (br, 2H), 6.89 (d, *J* = 8.71 Hz, 2H), 5.86 (br, 1H), 4.78 (s, 2H), 3.83 – 3.63 (m, 4H), 3.18 – 2.88 (m, 4H), 2.84 – 2.69 (m, 2H), 2.69 – 2.55 (m, 2H), 1.88 – 1.69 (m, 4H). ^{13}C NMR (101 MHz, DMSO) δ 167.0, 164.3, 160.4, 160.2, 147.2, 142.1, 139.4, 138.0, 136.6, 135.8, 132.2, 131.8, 130.1, 129.6, 127.6, 126.6, 122.0, 115.9, 66.6, 58.3, 49.5, 27.9, 25.3, 22.9, 22.2.; HRMS (ESI) *m/z* calculated for $C_{29}H_{32}N_7O_3S$ $[M+H]^+$: 558.2287, found: 558.2284, Purity 95%.

2-(3-{4-Amino-6-[(4-morpholinophenyl)amino]-1,3,5-triazin-2-yl}-2-(hydroxymethyl)phenyl)-5-(*t*-butyl)isoindolin-1-one (3h). To a solution of **22** (146 mg, 0.48 mmol) in DME (7.1 mL) was added **24h** (220mg, 0.48 mmol), $Pd(PPh_3)_4$ (27 mg, 0.024 mmol), K_2CO_3 (131mg, 0.95 mmol) and water (2.3 mL), and the mixture was stirred at 100°C for 4 hr. The reaction mixture was diluted with water (30 mL) and extracted with ethyl acetate (2×25 mL). The combined organic layers were washed successively with water (50 mL) and brine (50 mL), then the organic layers were dried over sodium sulfate, and concentrated. The crude material was purified by flash chromatography on silica gel, eluted with hexane/ethyl acetate to afford **3h** as pale-yellow powder (35mg, 0.062 mmol, 13%). ^{1}H NMR (400 MHz, DMSO-d_6) δ 9.53 (br, 1H), 7.93 – 7.44 (m, 8H), 7.30 (br, 2H), 6.90 (d, J = 8.49 Hz, 2H), 5.08 (br, 1H), 4.92 (s, 2H), 4.59 – 4.29 (m, 2H), 3.86 – 3.59 (m, 4H), 3.20 – 2.87 (m, 4H), 1.37 (s, 9H). ^{13}C NMR (101 MHz, DMSO) δ 173.2, 167.8, 166.9, 155.7, 147.3, 143.0, 140.4, 138.9, 138.7, 132.1, 130.8, 130.0, 129.6, 128.5, 125.9, 123.4, 122.1, 120.6, 115.9, 98.7, 66.6, 57.5, 54.7, 49.5, 35.6, 31.6.; HRMS (ESI) *m/z* calculated for $C_{32}H_{36}N_7O_3$ $[M+H]^+$: 566.2880, found: 566.2867, Purity 100%.

2-(3-{4-Amino-6-[(4-morpholinophenyl)amino]-1,3,5-triazin-2-yl}-2-(hydroxymethyl)phenyl)-6-cyclopropylphthalazin-1(*2H*)-one (3i). To a mixture of **24i** (112 mg, 0.24 mmol) and **22** (74.6 mg, 0.24 mmol) in DME (1.6 mL) was added a solution of K_2CO_3 (67 mg, 0.49 mmol) in water (0.4 mL), and degassed with N_2 for 5 min. To this mixture, $Pd(PPh_3)_4$ (28.1 mg, 0.024 mmol) was added, and the mixture was heated in the microwave reactor at 110 °C for 20 min. The reaction mixture was diluted with water (50 mL) and extracted with ethyl acetate (3×25 mL). The combined organic layers were washed successively with water (50 mL) and brine (50 mL), then dried over sodium sulfate. The solvent was evaporated to afford the corresponding acetyl-protected intermediate. The obtained intermediate was dissolved in

MeOH/THF (2:1, 6 mL), and K_2CO_3 (200 mg) were added to the solution. The mixture was stirred at room temperature for 16 hr. The reaction mixture was diluted with water (50 mL) and extracted with ethyl acetate (3×25 mL). The combined organic layers were washed successively with water (50 mL) and brine (50 mL), then dried over sodium sulfate, and concentrated. The crude residue was purified by flash chromatography on silica gel, eluted with hexane/ethyl acetate to afford **3i** as a pale-yellow powder (26 mg, 0.044 mmol, 18%). ^{1}H NMR (400 MHz, DMSO-d_6) δ 9.50 (br, 1H), 8.46 (s, 1H), 8.18 (d, J = 8.26 Hz, 1H), 7.87 (dd, J = 1.58, 7.64 Hz, 1H), 7.72 (d, J = 1.73 Hz, 1H), 7.69 – 7.50 (m, 4H), 7.49 (dd, J = 1.56, 7.86 Hz, 1H), 7.24 (br, 2H), 6.90 (d, J = 8.80 Hz, 2H), 5.06 (br, 1H), 4.42 (s, 1H), 4.30 (s, 1H), 3.82 – 3.66 (m, 4H), 3.11 – 2.98 (m, 4H), 2.26 – 2.12 (m, 1H), 1.20 – 1.11 (m, 2H), 0.99 – 0.82 (m, 2H). ^{13}C NMR (101 MHz, DMSO) δ 173.2, 169.2, 159.2, 153.0, 151.5, 147.3, 141.9, 140.2, 138.7, 137.9, 130.8, 130.4, 130.3, 128.6, 128.2, 127.8, 126.6, 125.4, 123.2, 115.9, 66.6, 57.1, 49.5, 40.4, 16.0, 11.4.; HRMS (ESI) *m/z* calculated for $C_{31}H_{31}N_8O_3$ $[M+H]^+$: 563.2519, found: 563.2516, Purity 97%.

Compounds **3j** and **3n** were synthesized from 6-chloro-N^2-(4-morpholinophenyl)-1,3,5-triazine-2,4-diamine (**22**) and the appropriate boronate esters **24j** and **25, respectively,** using a procedure similar to the procedure for the preparation of **3h**. Compounds **3k**, **3l** and **3m** were synthesized from **22** and the appropriate boronate esters **24k**, **24l** and **24m**, respectively, a procedure similar to the procedure for the preparation of **3i**.

2-(3-{4-Amino-6-[(4-morpholinophenyl)amino]-1,3,5-triazin-2-yl}-2-(hydroxymethyl)phenyl)-6-cyclopropyl-3,4-dihydroisoquinolin-1(*2H*)-one (3j). Off-white solids; 5.6% yield. ^{1}H NMR (400 MHz, DMSO-d_6) δ 9.50 (br, 1H), 7.86 – 7.70 (m, 2H), 7.61 (br, 2H), 7.52 – 7.38 (m, 2H), 7.26 (br, 2H), 7.14 – 7.03 (m, 2H), 6.95 – 6.80 (m, 2H), 5.08 (br, 1H), 4.61 – 4.47 (m, 1H), 4.42 – 4.27 (m, 1H), 4.00 – 3.79 (m, 2H), 3.81 – 3.67 (m, 4H), 3.28 –

3.15 (m, 2H), 3.13 – 2.96 (m, 4H), 2.06 – 1.92 (m, 1H), 1.09 – 0.97 (m, 2H), 0.82 – 0.70 (m, 2H). ^{13}C NMR (101 MHz, DMSO) δ 177.9, 176.4, 165.8, 165.4, 164.0, 153.4, 149.2, 140.4, 139.6, 137.9, 132.1, 130.3, 128.2, 124.5, 124.3, 121.8, 115.9, 115.6, 113.8, 109.7, 66.6, 57.6, 50.4, 49.5, 28.1, 15.8, 10.6.; HRMS (ESI) *m/z* calculated for $C_{32}H_{34}N_7O_3$ $[M+H]^+$: 564.2723, found: 564.2705, Purity 98%.

2-[2-(3-{4-Amino-6-[(4-morpholinophenyl)amino]-1,3,5-triazin-2-yl}-2-(hydroxymethyl)phenyl)-8-fluoro-1-oxo-1,2,3,4-tetrahydroisoquinolin-6-yl]-2-methylpropanenitrile (3k). A pale-yellow powder; 74% yield. ^{1}H NMR (400 MHz, DMSO-d_6) δ 9.61 (br, 1H), 7.75 (dd, J = 2.32, 6.83 Hz, 1H), 7.61 (br, 2H), 7.54 – 7.44 (m, 2H), 7.43 (d, J = 1.86 Hz, 1H), 7.39 – 7.21 (m, 3H), 6.91 (d, J = 8.83 Hz, 2H), 4.60 (d, J = 12.04 Hz, 1H), 4.37 (d, J = 12.02 Hz, 1H), 4.01 – 3.77 (m, 2H), 3.76 – 3.68 (m, 4H), 3.37 – 3.13 (m, 2H), 3.10 – 3.01 (m, 4H), 1.74 (s, 6H). ^{13}C NMR (101 MHz, DMSO) δ 163.3, 160.7, 160.3, 147.8, 147.7, 147.4, 143.7, 143.1, 138.0, 130.4, 129.6, 128.7, 124.3, 122.1, 120.9, 117.2, 117.2, 115.9, 113.2, 112.9, 110.0, 66.6, 57.6, 50.1, 49.5, 37.3, 28.9, 28.3.; HRMS (ESI) *m/z* calculated for $C_{33}H_{34}FN_8O_3$ $[M+H]^+$: 609.2738, found: 609.2737, Purity 97%.

2-(3-{4-Amino-6-[(4-morpholinophenyl)amino]-1,3,5-triazin-2-yl}-2-(hydroxymethyl)phenyl)-6-cyclopropyl-8-fluoro-3,4-dihydroisoquinolin-1(*2H*)-one (3l). Off-white solids; 63% yield. ^{1}H NMR (400 MHz, DMSO-d_6) δ 9.50 (br, 1H), 7.76 (dd, J = 1.81, 7.34 Hz, 1H), 7.73 – 7.53 (m, 2H), 7.53 – 7.36 (m, 2H), 7.26 (br, 2H), 7.03 – 6.75 (m, 4H), 5.07 (br, 1H), 4.68 – 4.49 (m, 1H), 4.44 – 4.24 (m, 1H), 3.94 – 3.77 (m, 2H), 3.76 – 3.69 (m, 4H), 3.28 – 3.08 (m, 2H), 3.08 – 2.94 (m, 4H), 2.06 – 1.92 (m, 1H), 1.11 – 0.98 (m, 2H), 0.88 – 0.75 (m, 2H). ^{13}C NMR (101 MHz, DMSO) δ 173.2, 166.9, 164.4, 163.5, 160.9, 151.7, 147.3, 143.4, 142.6, 140.4, 138.0, 132.1, 130.4, 129.6, 128.6, 122.0, 120.6, 115.9, 114.7, 112.4, 66.6, 57.7,

50.2, 49.5, 28.9, 15.7, 11.0, 11.0.; HRMS (ESI) *m/z* calculated for $C_{32}H_{33}FN_7O_3$ $[M+H]^+$: 582.2629, found: 582.2628, Purity 98%.

2-(3-{4-Amino-6-[(4-morpholinophenyl)amino]-1,3,5-triazin-2-yl}-2-(hydroxymethyl)phenyl)-6-cyclopropyl-8-fluoroisoquinolin-1(*2H*)-one (3m). Off-white solids; 68% yield. ^{1}H NMR (400 MHz, DMSO-d_6) δ 9.55 (br, 1H), 7.90 (dd, *J* = 1.43, 7.81 Hz, 1H), 7.73 – 7.59 (m, 2H), 7.56 (t, *J* = 7.80 Hz, 1H), 7.45 (dd, *J* = 1.43, 7.95 Hz, 1H), 7.42 – 7.14 (m, 4H), 6.99 (dd, *J* = 1.63, 13.17 Hz, 1H), 6.95 – 6.86 (m, 2H), 6.62 (dd, *J* = 2.09, 7.55 Hz, 1H), 5.14 (br, 1H), 4.54 (dd, *J* = 4.98, 12.14 Hz, 1H), 4.13 (dd, *J* = 8.88, 12.12 Hz, 1H), 3.81 – 3.66 (m, 4H), 3.12 – 2.98 (m, 4H), 2.14 – 2.00 (m, 1H), 1.14 – 1.05 (m, 2H), 0.92 – 0.81 (m, 2H). ^{13}C NMR (101 MHz, DMSO) δ 173.0, 163.7, 161.1, 158.8, 152.3, 147.3, 141.1, 140.5, 140.4, 137.8, 135.4, 132.1, 130.8, 130.7, 128.7, 122.1, 118.9, 115.9, 112.4, 111.4, 111.2, 104.7, 66.6, 57.2, 49.5, 15.9, 11.2.; HRMS (ESI) *m/z* calculated for $C_{32}H_{31}FN_7O_3$ $[M+H]^+$: 580.2472, found: 580.2482, Purity 97%.

2-(3-{4-Amino-6-[(4-morpholinophenyl)amino]-1,3,5-triazin-2-yl}-2-(hydroxymethyl)phenyl)-7,7-dimethyl-2,3,4,6,7,8-hexahydro-*1H*-cyclopenta[4,5]pyrrolo[1,2-a]pyrazin-1-one (3n). Off-white solids; 11% yield. ^{1}H NMR (400 MHz, DMSO-d_6) δ 9.48 (br, 1H), 7.74 (dd, *J* = 1.78, 7.38 Hz, 1H), 7.69 – 7.50 (m, 2H), 7.50 – 7.38 (m, 2H), 7.25 (br, 2H), 6.94 – 6.83 (m, 2H), 6.57 – 6.43 (m, 1H), 5.04 (br, 1H), 4.54 (d, *J* = 11.55 Hz, 1H), 4.42 – 4.31 (m, 1H), 4.25 – 4.14 (m, 2H), 4.09 – 3.97 (m, 1H), 3.97 – 3.85 (m, 1H), 3.80 – 3.66 (m, 4H), 3.11 – 2.98 (m, 4H), 2.56 (s, 2H), 2.42 (s, 2H), 1.24 – 1.19 (m, 6H). ^{13}C NMR (101 MHz, DMSO) δ 159.1, 147.3, 142.9, 140.5, 140.3, 138.3, 132.1, 132.0, 131.9, 130.5, 129.5, 129.2, 128.4, 126.9, 125.5, 122.1, 115.9, 108.5, 66.6, 57.5, 50.3, 49.5, 45.8, 42.4,

41.3, 39.5, 30.6, 30.6.; HRMS (ESI) *m/z* calculated for $C_{32}H_{37}N_8O_3$ $[M+H]^+$: 581.2989, found: 581.2993, Purity 100%.

2-(3-{4-[(*1H*-Pyrazol-4-yl)amino]-6-amino-1,3,5-triazin-2-yl}-2-(hydroxymethyl)phenyl)-6-cyclopropyl-8-fluoroisoquinolin-1(*2H*)-one (4a). To a mixture of chlorotriazine **26a** (124 mg, 0.42 mmol) and boronate ester **24m** (200 mg, 0.419 mmol) in DME (6 mL) was added a solution of K_2CO_3 (116 mg, 0.84 mmol) in water (2 mL), and the mixture was degassed with N_2 for 5 min. $Pd(PPh_3)_4$ (24.21 mg, 0.021 mmol) was added to the mixture, and the mixture was heated in the microwave reactor at 110 °C for 10 min. The reaction mixture diluted with added water (50 mL) and extracted with ethyl acetate (3×25 mL). The combined organic layers were washed successively with water (50 mL) and brine (50 mL), then dried over sodium sulfate. The solvent was evaporated, and the residue was purified by flash chromatography on silica gel, eluted with hexane/ethyl acetate to afford the corresponding acetylated product as a crude mixture. To a solution of the obtained crude product in MeOH (10 mL), *p*-toluenesulfonic acid monohydrate (179 mg, 0.94 mmol) was added, and the mixture was stirred at 60°C for 1 hr. After cooling to room temperature, the resulting solids were collected by filtration, and washed successively with water and diethyl ether to give colorless solids. The obtained solids were dissolved in MeOH (7 mL), and K_2CO_3 (100 mg) was added to the solution. The mixture was stirred at room temperature for 3 hr. The resulting solids were collected by filtration, and washed successively with water and diethyl ether to afford **4a** as colorless solids (150 mg, 0.30 mmol, 81%). ^{1}H NMR (400 MHz, DMSO-d_6) δ 12.55 (s, 1H), 9.71 (s, 1H), 8.16 – 7.59 (m, 3H), 7.61 – 7.51 (m, 1H), 7.45 (dd, *J* = 1.45, 7.82 Hz, 1H), 7.38 – 7.31 (m, 3H), 7.29 – 7.22 (m, 1H), 7.00 (dd, *J* = 1.72, 13.32 Hz, 1H), 6.67 – 6.56 (m, 1H), 5.33 – 4.93 (m, 1H), 4.60 – 4.40 (m, 1H), 4.18 – 4.01 (m, 1H), 2.15 – 2.00 (m, 1H), 1.17 – 1.03 (m, 2H), 0.93 – 0.81 (m, 2H). ^{13}C NMR (101

MHz, DMSO) δ 172.7, 167.2, 163.7, 163.3, 161.1, 158.8, 158.7, 152.3, 141.1, 140.5, 140.4, 137.8, 135.4, 130.8, 128.6, 122.1, 118.9, 112.4, 111.4, 111.2, 104.6, 57.2, 15.9, 11.2.; HRMS (ESI) *m/z* calculated for $C_{25}H_{22}FN_8O_2$ $[M+H]^+$: 485.1850, found: 485.1842, Purity 97%.

2-(3-{4-Amino-6-[(1-methyl-*1H*-pyrazol-4-yl)amino]-1,3,5-triazin-2-yl}-2-(hydroxymethyl)phenyl)-6-cyclopropyl-8-fluoroisoquinolin-1(*2H*)-one (4b). To a mixture of boronate ester **24m** (141 mg, 0.30 mmol) and chlorotriazine **26b** (67 mg, 0.30 mmol) in DME (5 mL) was added a solution of K_2CO_3 (82 mg, 0.59 mmol) in water (1.6 mL), and the mixture was degassed with N_2 for 5 min. $Pd(PPh_3)_4$ (17 mg, 0.015 mmol) was added to the mixture, and the mixture was heated in the microwave reactor at 110 °C for 20 min. The reaction mixture was diluted with water (50 mL) and extracted with ethyl acetate (3×25 mL). The combined organic layers were washed successively with water (50 mL) and brine (50 mL), then dried over sodium sulfate, and concentrated. The residue was purified by flash chromatography on silica gel, eluted with hexane/ethyl acetate to afford the corresponding acetylated product as a crude mixture. To a solution of the obtained crude product in MeOH (5 mL), K_2CO_3 (100mg) was added, and the mixture was stirred at room temperature for 2 hr. The reaction mixture was diluted with water (50 mL) and the resulting solids were collected by filtration, and washed successively with water and diethyl ether to afford **4b** as off-white solids (85 mg, 0.17 mmol, 57%). ^{1}H NMR (400 MHz, DMSO-d_6) δ 9.70 (s, 1H), 8.09 – 7.77 (m, 2H), 7.62 – 7.41 (m, 3H), 7.37 – 7.25 (m, 4H), 7.00 (dd, *J* = 1.68, 13.25 Hz, 1H), 6.62 (dd, *J* = 2.08, 7.52 Hz, 1H), 5.19 (dd, *J* = 5.00, 9.08 Hz, 1H), 4.49 (dd, *J* = 5.05, 12.12 Hz, 1H), 4.14 – 4.04 (m, 1H), 3.79 (s, 3H), 2.14 – 2.02 (m, 1H), 1.17 – 1.01 (m, 2H), 0.92 – 0.83 (m, 2H). ^{13}C NMR (101 MHz, DMSO) δ 172.7, 167.2, 163.7, 163.3, 161.1, 158.8, 152.3, 141.2, 140.5, 140.4, 137.8, 135.4, 130.9, 130.7, 128.6, 122.7, 121.9, 118.9,

112.4, 111.3, 104.7, 57.2, 39.2, 15.9, 11.2.; HRMS (ESI) *m/z* calculated for $C_{26}H_{24}FN_8O_2$ $[M+H]^+$: 499.2006, found: 499.2011, Purity 100%.

Compounds **4c**, **4d**, **4e**, **4f**, **4g**, **4h** and **4i** were synthesized from 2-(6-cyclopropyl-8-fluoro-1-oxoisoquinolin-2(1*H*)-yl)-6-(4,4,5,5-tetramethyl-1,3,2-dioxaborolan-2-yl)benzyl acetate (**24m**) and the appropriate chlorotriazines **26c**, **26d**, **26e**, **26f**, **26g**, **26h** and **26i**, respectively, using a procedure similar to the procedure for the preparation of **4b**.

2-(3-{4-Amino-6-[(1-cyclopropyl-*1H*-pyrazol-4-yl)amino]-1,3,5-triazin-2-yl}-2-(hydroxymethyl)phenyl)-6-cyclopropyl-8-fluoroisoquinolin-1(*2H*)-one (4c). Colorless solids; 75% yield. ^{1}H NMR (400 MHz, DMSO-d_6) δ 9.73 (s, 1H), 8.11 (s, 1H), 7.99 – 7.83 (m, 1H), 7.70 – 7.50 (m, 2H), 7.50 – 7.42 (m, 1H), 7.38 (br, 2H), 7.34 (d, *J* = 7.34 Hz, 1H), 7.31 – 7.21 (m, 1H), 7.00 (dd, *J* = 1.65, 13.24 Hz, 1H), 6.62 (dd, *J* = 2.06, 7.53 Hz, 1H), 5.22 (dd, *J* = 5.09, 9.10 Hz, 1H), 4.51 (dd, *J* = 5.03, 12.10 Hz, 1H), 4.11 (dd, *J* = 9.16, 12.21 Hz, 1H), 3.75 – 3.59 (m, 1H), 2.16 – 2.01 (m, 1H), 1.19 – 0.69 (m, 8H). ^{13}C NMR (101 MHz, DMSO) δ 172.7, 167.1, 163.7, 163.2, 161.1, 158.8, 152.3, 141.1, 140.5, 140.3, 137.8, 135.4, 130.8, 130.8, 128.6, 122.4, 121.0, 118.9, 112.4, 111.3, 104.7, 57.2, 33.2, 15.9, 11.2, 6.7.; HRMS (ESI) *m/z* calculated for $C_{28}H_{26}FN_8O_2$ $[M+H]^+$: 525.2163, found: 525.2160, Purity 99%.

2-[3-(4-Amino-6-{[1-(1-cyclopropylethyl)-*1H*-pyrazol-4-yl]amino}-1,3,5-triazin-2-yl)-2-(hydroxymethyl)phenyl]-6-cyclopropyl-8-fluoroisoquinolin-1(*2H*)-one (4d). Colorless solids; 83% yield. ^{1}H NMR (400 MHz, DMSO-d_6) δ 9.74 (s, 1H), 8.13 (s, 1H), 8.02 – 7.95 (m, 1H), 7.91 (dd, *J* = 1.45, 7.88 Hz, 1H), 7.67 – 7.50 (m, 2H), 7.52 – 7.42 (m, 1H), 7.42 – 7.30 (m, 2H), 7.29 – 7.22 (m, 1H), 7.00 (dd, *J* = 1.64, 13.24 Hz, 1H), 6.70 – 6.56 (m, 1H), 5.18 (br, 1H), 4.69 – 4.41 (m, 1H), 4.30 – 3.97 (m, 1H), 3.69 – 3.51 (m, 1H), 2.13 – 2.01 (m, 1H), 1.57 – 1.42 (m, 3H), 1.31 – 1.14 (m, 1H), 1.14 – 1.04 (m, 2H), 0.92 – 0.83 (m, 2H), 0.63 – 0.51 (m, 1H), 0.50 –

0.38 (m, 1H), 0.39 – 0.26 (m, 2H). ^{13}C NMR (101 MHz, DMSO) δ 172.7, 168.7, 167.1, 163.3, 161.1, 158.8, 153.8, 152.2, 141.1, 140.5, 137.8, 135.4, 130.7, 130.5, 128.6, 122.1, 119.3, 118.9, 112.4, 112.4, 104.7, 62.4, 57.3, 21.0, 17.9, 15.9, 11.2, 4.3, 4.0.; HRMS (ESI) *m/z* calculated for $C_{30}H_{30}FN_8O_2$ $[M+H]^+$: 553.2476, found: 553.2452, Purity 100%.

4-({4-Amino-6-[3-(6-cyclopropyl-8-fluoro-1-oxoisoquinolin-2(*1H*)-yl)-2-(hydroxymethyl)phenyl]-1,3,5-triazin-2-yl}amino)-1-methyl-*1H*-pyrrole-2-carbonitrile (4e). Off-white solids; 37% yield. ^{1}H NMR (400 MHz, DMSO-d_6) δ 9.81 (s, 1H), 7.99 – 7.79 (m, 1H), 7.65 – 7.49 (m, 2H), 7.49 – 7.19 (m, 5H), 7.13 – 6.83 (m, 2H), 6.62 (dd, *J* = 2.09, 7.53 Hz, 1H), 5.25 – 4.95 (m, 1H), 4.62 – 4.40 (m, 1H), 4.22 – 3.93 (m, 1H), 3.75 (s, 3H), 2.15 – 2.00 (m, 1H), 1.16 – 1.04 (m, 2H), 0.93 – 0.81 (m, 2H). ^{13}C NMR (101 MHz, DMSO) δ 172.8, 167.1, 163.5, 161.1, 158.8, 152.3, 141.2, 140.5, 140.3, 137.8, 135.4, 130.8, 128.6, 124.6, 119.8, 118.9, 114.4, 112.4, 111.4, 111.4, 111.2, 104.7, 101.1, 57.2, 35.7, 15.9, 11.2.; HRMS (ESI) *m/z* calculated for $C_{28}H_{24}FN_8O_2$ $[M+H]^+$: 523.2006, found: 523.2003, Purity 100%.

4-({4-Amino-6-[3-(6-cyclopropyl-8-fluoro-1-oxoisoquinolin-2(*1H*)-yl)-2-(hydroxymethyl)phenyl]-1,3,5-triazin-2-yl}amino)-1-ethyl-*1H*-pyrrole-2-carbonitrile (4f). Off-white solids; 79% yield. ^{1}H NMR (400 MHz, DMSO-d_6) δ 9.81 (s, 1H), 7.88 (d, *J* = 7.81 Hz, 1H), 7.67 – 7.49 (m, 2H), 7.51 – 7.41 (m, 1H), 7.42 – 7.30 (m, 3H), 7.30 – 7.22 (m, 1H), 7.08 – 6.95 (m, 2H), 6.62 (dd, *J* = 2.11, 7.48 Hz, 1H), 5.25 – 5.10 (m, 1H), 4.63 – 4.43 (m, 1H), 4.22 – 3.97 (m, 3H), 2.15 – 1.99 (m, 1H), 1.49 – 1.28 (m, 3H), 1.16 – 1.05 (m, 2H), 0.93 – 0.81 (m, 2H). ^{13}C NMR (101 MHz, DMSO) δ 172.8, 167.1, 163.5, 161.1, 158.8, 152.3, 141.2, 140.5, 140.3, 137.8, 135.4, 130.8, 129.2, 128.7, 124.7, 118.9, 118.1, 114.4, 112.4, 111.6, 111.3, 104.7, 99.9, 57.2, 43.9, 16.8, 15.9, 11.2.; HRMS (ESI) *m/z* calculated for $C_{29}H_{26}FN_8O_2$ $[M+H]^+$: 537.2163, found: 537.2164, Purity 100%.

4-({4-Amino-6-[3-(6-cyclopropyl-8-fluoro-1-oxoisoquinolin-2(*1H*)-yl)-2-(hydroxymethyl)phenyl]-1,3,5-triazin-2-yl}amino)-1-isopropyl-*1H*-pyrrole-2-carbonitrile (4g). Off-white solids; 33% yield. ^{1}H NMR (400 MHz, DMSO-d_6) δ 9.79 (s, 1H), 7.88 (d, J = 7.65 Hz, 1H), 7.67 (s, 1H), 7.62 – 7.50 (m, 1H), 7.48 – 7.43 (m, 1H), 7.40 (br, 2H), 7.33 (d, J = 7.38 Hz, 1H), 7.31 – 7.24 (m, 1H), 7.05 – 6.95 (m, 2H), 6.66 – 6.57 (m, 1H), 5.17 (s, 1H), 4.66 – 4.33 (m, 2H), 4.19 – 4.00 (m, 1H), 2.15 – 2.00 (m, 1H), 1.48 (d, J = 6.63 Hz, 6H), 1.14 – 1.06 (m, 2H), 0.92 – 0.82 (m, 2H). ^{13}C NMR (101 MHz, DMSO) δ 163.7, 163.3, 140.6, 140.3, 135.4, 130.8, 130.7, 128.7, 118.9, 115.2, 114.5, 113.8, 112.4, 111.5, 111.4, 106.2, 105.1, 104.7, 100.0, 99.3, 87.5, 82.4, 78.1, 51.9, 51.3, 23.4, 15.9, 11.2.; HRMS (ESI) *m/z* calculated for $C_{30}H_{28}FN_8O_2$ $[M+H]^+$: 551.2319, found: 551.2310, Purity 100%.

4-({4-Amino-6-[3-(6-cyclopropyl-8-fluoro-1-oxoisoquinolin-2(*1H*)-yl)-2-(hydroxymethyl)phenyl]-1,3,5-triazin-2-yl}amino)-1-cyclopropyl-*1H*-pyrrole-2-carbonitrile (4h). Off-white solids; 16% yield. ^{1}H NMR (400 MHz, DMSO-d_6) δ 9.79 (br, 1H), 7.90 (d, J = 7.75 Hz, 1H), 7.64 – 7.50 (m, 2H), 7.52 – 7.37 (m, 3H), 7.34 (d, J = 7.36 Hz, 1H), 7.27 (d, J = 1.66 Hz, 1H), 7.06 – 6.85 (m, 2H), 6.62 (dd, J = 2.08, 7.46 Hz, 1H), 5.20 (br, 1H), 4.66 – 4.41 (m, 1H), 4.25 – 4.03 (m, 1H), 3.63 – 3.46 (m, 1H), 2.15 – 2.01 (m, 1H), 1.17 – 0.96 (m, 6H), 0.92 – 0.83 (m, 2H). ^{13}C NMR (101 MHz, DMSO) δ 172.7, 167.1, 163.7, 163.3, 161.1, 158.8, 152.3, 141.2, 140.5, 140.3, 137.9, 135.3, 130.8, 128.6, 124.3, 118.9, 118.5, 114.4, 112.4, 112.2, 111.3, 104.7, 102.1, 57.2, 30.0, 15.9, 11.2, 7.0.; HRMS (ESI) *m/z* calculated for $C_{30}H_{26}FN_8O_2$ $[M+H]^+$: 549.2163, found: 549.2139, Purity 100%.

4-({4-Amino-6-[3-(6-cyclopropyl-8-fluoro-1-oxoisoquinolin-2(*1H*)-yl)-2-(hydroxymethyl)phenyl]-1,3,5-triazin-2-yl}amino)-1-[2-(2-methoxyethoxy)ethyl]-*1H*-pyrrole-2-carbonitrile (4i). Off-white solids; 69% yield. ^{1}H NMR (400 MHz, DMSO-d_6) δ 9.82

(s, 1H), 8.02 – 7.83 (m, 1H), 7.67 – 7.22 (m, 7H), 7.10 (d, *J* = 1.90 Hz, 1H), 6.99 (dd, *J* = 1.64, 13.20 Hz, 1H), 6.62 (dd, *J* = 2.09, 7.57 Hz, 1H), 5.27 – 5.10 (m, 1H), 4.62 – 4.44 (m, 1H), 4.24 – 4.04 (m, 3H), 3.83 – 3.63 (m, 2H), 3.57 – 3.46 (m, 2H), 3.47 – 3.35 (m, 2H), 3.23 (s, 3H), 2.14 – 2.01 (m, 1H), 1.15 – 1.04 (m, 2H), 0.92 – 0.83 (m, 2H). ^{13}C NMR (101 MHz, DMSO) δ 172.8, 167.1, 163.5, 161.1, 158.8, 152.3, 141.2, 140.5, 140.3, 137.8, 135.4, 130.8, 130.7, 128.6, 124.8, 118.9, 118.7, 114.4, 112.4, 111.7, 111.3, 104.7, 101.0, 71.7, 70.1, 70.1, 58.6, 57.2, 48.9, 15.9, 11.2.; HRMS (ESI) *m/z* calculated for $C_{32}H_{32}FN_8O_4$ requires $[M+H]^+$: 611.2531, found: 611.2533, Purity 96%.

4-(*t*-Butyl)-*N*-[2-methyl-3-(4,4,5,5-tetramethyl-1,3,2-dioxaborolan-2-yl)phenyl]benzamide (6). Under nitrogen atmosphere, 2-Methyl-3-(4,4,5,5-tetramethyl-1,3,2-dioxaborolan-2-yl)aniline **5** (326 mg, 1.49 mmol) was dissolved in DCM (15 mL) and cooled with an ice bath. To this solution, pyridine (0.132 mL, 1.64 mmol) and 4-*t*-butylbenzoyl chloride (439 mg, 2.23 mmol) were added dropwise and the mixture was stirred at room temperature for 4 h. The reaction mixture was diluted with chloroform (75 mL), washed successively with water (2×30 mL), 1N hydrochloric acid solution (30 mL), saturated $NaHCO_3$ aq. (30 mL) and brine (30 mL), then the organic layer was dried over sodium sulfate, filtered and concentrated to afford **6** (565 mg, 1.44 mmol, 97%). ^{1}H NMR (400 MHz, DMSO-d_6) δ 9.80 (s, 1H), 7.92 (d, *J* = 8.3 Hz, 2H), 7.54 (m, 3H), 7.39 (d, *J* = 7.6 Hz, 1H), 7.21 (t, *J* = 7.6 Hz, 1H), 2.37 (s, 3H), 1.32 (s, 9H), 1.32 (s, 12H). ; LCMS (*m/z*): mass was calculated for $C_{24}H_{32}BNO_3$ requires 393.2, found 394.0 $[M+H]^+$.

{4-[(6-Chloropyrazin-2-yl)amino]phenyl}(morpholino)methanone (8). A mixture of 2,6-dichloropyrazine (250 mg, 1.68 mmol) and (4-aminophenyl)morpholin-4-ylmethanone **7** (345 mg, 1.68 mmol) in toluene (8 mL) was degassed with N_2 gas for 5 min. Pd_2dba_3 (15 mg, 0.017 mmol) was added to the solution and the mixture was degassed again with N_2 for 5 min. To this

mixture, sodium t-butoxide (322 mg, 3.35 mmol) was added, and the mixture was degassed with N_2 for 2 min and then heated at 90 °C for 16 h. The solvent was evaporated, and the residue was dissolved in acetone, filtered through celite. The filtrate was concentrated and the residue was purified by flash column chromatography using 50% ethyl acetate in hexane as eluent to afford **8** (210 mg, 0.66 mmol, 39%). ^{1}H NMR (400 MHz, DMSO-d_6) δ 10.08 (s, 1H), 8.22 (s, 1H), 8.05 (s, 1H), 7.70 (d, J = 8.6 Hz, 2H), 7.43 (d, J = 8.6 Hz, 2H), 3.60-3.48 (m, 8H).; LCMS (*m/z*): mass was calculated for $C_{15}H_{15}ClN_4O_2$ requires 318.1, found 318.8 $[M+H]^+$.

{4-[(4-Chloro-1,3,5-triazin-2-yl)amino]phenyl}(morpholino)methanone (9c). A solution of 2,4-dichloro-1,3,5-triazine (300 mg, 2.0 mmol) in DMF (5 mL) was cooled with an ice bath, and DIEA (0.5 mL, 3.0 mmol) and (4-aminophenyl)morpholin-4-ylmethanone (412 mg, 2.0 mmol) were added to the solution, and the mixture was then stirred at 0 °C for 16 h. The reaction mixture was diluted with water (15 mL), and extracted with ethyl acetate (3×50 mL). The combined organic layers were washed with water (20 mL), dried over sodium sulfate, filtered and concentrated. The crude material was purified by chromatography on silica gel, eluted with hexane/ethyl acetate to afford **9c** (270 mg, 0.84 mmol, 42%). ^{1}H NMR (400 MHz, DMSO-d_6) δ 10.94 (s, 1H), 8.69 (s, 1H), 7.75 (d, J = 7.71 Hz, 3H), 7.44 (d, J = 8.52 Hz, 2H), 3.77 – 3.35 (m, 8H).; LCMS (*m/z*): mass was calculated for $C_{14}H_{14}ClN_5O_2$ requires 319.1, found 319.8 $[M+H]^+$.

{**4-[(4-Chloro-6-methyl-1,3,5-triazin-2-yl)amino]phenyl}(morpholino)methanone (9d)**. Following the procedures described for **9c**, 2,4-dichloro-6-methyl-1,3,5-triazine (200 mg, 1.22 mmol) and (4-aminophenyl)morpholin-4-ylmethanone (252 mg, 1.22 mmol) were used for synthesis of **9d** (120 mg, 0.36 mmol, 29.5 %). ^{1}H NMR (400 MHz, DMSO-d_6) δ 10.83 (s, 1H), 7.76 (br, 2H), 7.43 (d, J = 8.5 Hz, 2H), 3.76 – 3.34 (m, 8H), 2.44 (s, 3H).

{4-[(4-Amino-6-chloro-1,3,5-triazin-2-yl)amino]phenyl}(morpholino)methanone (9e). Following the procedures described for **9c**, 2-amino-4,6-dichloro-1,3,5-triazine (200 mg, 1.21 mmol) and (4-aminophenyl)morpholin-4-ylmethanone (250 mg, 1.21 mmol) were used for synthesis of **9e** (325 mg, 0.97 mmol, 80 %). ^{1}H NMR (400 MHz, DMSO-d_6) δ 10.15 (s, 1H), 7.81 (d, J = 8.3 Hz, 2H), 7.68 (br, 2H), 7.40 – 7.32 (m, 2H), 3.60 (br, 4H), 3.49 (br, 4H).

{4-[(4-Chloro-6-methoxy-1,3,5-triazin-2-yl)amino]phenyl}(morpholino)methanone (9f). A solution of 2,4-dichloro-6-methoxy-1,3,5-triazine (200 mg, 1.11 mmol) in MeOH (2.8 mL) was cooled with an ice bath, and DIEA (0.21 mL, 1.22 mmol) and (4-aminophenyl)morpholin-4-ylmethanone (229 mg, 1.11 mmol) were added to the solution, and the mixture was then stirred at 0 °C for 10 min. The reaction mixture was diluted with water (30 mL), extracted with ethyl acetate (2×25 mL). The combined organic layers were washed with water (20 mL) and brine (30 mL), dried over sodium sulfate, filtered and concentrated. The crude material was purified by flash chromatography on silica gel, eluted with hexane/ethyl acetate to afford **9f** (138 mg, 0.395 mmol, 35.5%). ^{1}H NMR (400 MHz, DMSO-d_6) (400 MHz, DMSO) δ 10.85 (s, 1H), 7.76 (br, 2H), 7.58 – 7.28 (m, 2H), 3.97 (s, 3H), 3.60 (br, 4H), 3.49 (br, 4H).

Methyl 3-[4-(*t*-butyl)benzamido]-2-methylbenzoate (11). To a solution of methyl 3-amino-2-methylbenzoate **10** (2.7 g, 16.4 mmol) in DCM (50 mL) was added TEA (4.6 mL, 37.7 mmol) and cooled with an ice bath. To this solution, 4-*t*-butylbenzoyl chloride (3.5 mL, 17.9 mmol) was added dropwise, and the mixture was stirred at room temperature for 3.5 h. The reaction mixture was diluted with DCM (30 mL), and washed successively with 1N hydrochloric acid solution (2×40 mL), water (40 mL), saturated $NaHCO_3$ aq. (2×40 mL) and brine (30 mL), then the organic layer was dried over sodium sulfate, and concentrated. The obtained crude solids were triturated with ether (50 mL) and hexane (50 mL) to afford **11** (4.5 g, 13.83mmol, 85%). ^{1}H

NMR (400 MHz, DMSO-d_6) δ 9.98 (s, 1H), 7.93 (d, J = 8.35 Hz, 2H), 7.65 (dd, J = 1.35, 7.85 Hz, 1H), 7.55 (d, J = 8.40 Hz, 2H), 7.53 – 7.49 (m, 1H), 7.34 (t, J = 7.82 Hz, 1H), 3.85 (s, 3H), 2.34 (s, 3H), 1.33 (s, 9H).

3-[4-(*t*-Butyl)benzamido]-2-methylbenzoic acid (12). To a solution of **11** (300 mg, 0.92 mmol) in MeOH/THF (1:1, 6 mL) was added 1 N NaOH aqueous (3 mL), and the mixture was stirred for 4 hr at room temperature. After removal of the solvent, the residue was diluted with water (20 mL), and washed with ethyl acetate (2×30 mL). The aqueous layer was acidified (~ pH 2) with 2N HCl. The resulting solids were collected by filtration, and washed with water (2×10 mL), and then dried to afford **12** (300 mg, quantitative yield). ^{1}H NMR (400 MHz, DMSO-d_6) δ 12.97 (br, 1H), 9.96 (s, 1H), 7.93 (d, J = 8.36 Hz, 2H), 7.69 – 7.62 (m, 1H), 7.58 – 7.51 (m, 2H), 7.51 – 7.44 (m, 1H), 7.31 (t, J = 7.81 Hz, 1H), 2.37 (s, 3H), 1.32 (s, 9H).

3-[4-(*t*-Butyl)benzamido]-*N*-methoxy-*N*,2-dimethylbenzamide (13). To a solution of **12** (0.5 g, 1.606 mmol) in DMF (5.8 mL) was added 1-(3-dimethylaminopropyl)-3-ethylcarbodiimide hydrochloride (0.37 g, 1.93 mmol) and 1-hydroxybenzotriazole monohydrate (0.3 g, 1.93 mmol), and the mixture was stirred for 1hr at room temperature. Then, TEA (0.56 ml, 4.01 mmol) and *N,O*-dimethylhydroxylamine hydrochloride (0.4 g, 4.01 mmol) were added to the mixture, and the stirring was continued for 16hr at room temperature. The reaction mixture was diluted with water, and extracted with ethyl acetate (3×25 mL). The combined the organic layers were washed successively with water (40 mL), 1 N NaOH (40 mL) and brine (40 mL), and dried over sodium sulfate. The solvent was evaporated to afford **13** (570 mg, 1.58 mmol, quantitative yield). ^{1}H NMR (400 MHz, DMSO-d_6) δ 9.88 (s, 1H), 7.93 (d, J = 8.46 Hz, 2H), 7.54 (d, J = 8.41 Hz, 2H), 7.39 (d, J = 7.68 Hz, 1H), 7.28 (t, J = 7.71 Hz, 1H), 7.17 (d, J = 7.46 Hz, 1H), 3.45 (br, 3H), 3.26 (br, 3H), 2.12 (s, 3H), 1.32 (s, 9H).

***N*-(3-Acetyl-2-methylphenyl)-4-(*t*-butyl)benzamide (14)**. A solution of **13** (0.5 g, 1.41mmol) in THF (14 mL) was cooled to 0°C, then 3M methyl magnesium bromide in diethyl ether (3.8 mL, 11.28 mmol) was added dropwise to the solution, and the mixture was stirred for 2hr at room temperature. The reaction was quenched with 1N HCl (40 mL), and extracted with ethyl acetate (3×25 mL). The combined organic layers were washed successively with water (40 mL), saturated $NaHCO_3$ aq. (40 mL) and brine (40 mL), and dried over sodium sulfate. The solvent was evaporated, and the residue was purified by flash chromatography on silica gel, eluted with hexane/ethyl acetate to afford **14** (212 mg, 0.685 mmol, 48.6 % yield). ^{1}H NMR (400 MHz, DMSO-d_6) δ 9.93 (s, 1H), 7.92 (d, J = 8.57 Hz, 2H), 7.67 – 7.60 (m, 1H), 7.55 (d, J = 8.59 Hz, 2H), 7.49 – 7.44 (m, 1H), 7.34 (t, J = 7.77 Hz, 1H), 2.57 (s, 3H), 2.25 (s, 3H), 1.32 (s, 9H).

4-(*t*-Butyl)-*N*-{2-methyl-3-[3-(methylthio)-1,2,4-triazin-5-yl]phenyl}benzamide (15). To a solution of **14** (0.3 g, 0.97 mmol) in 1,4-dioxane (3 mL) was added selenium oxide (0.14 g, 1.26 mmol) and water (0.1 mL), and the mixture was stirred for 18hr at 100 °C. The reaction mixture was filtered through a bed of celite to remove insoluble materials. The solvent was replaced with ethanol (5 mL), and Na_2CO_3 (0.15 g, 1.45 mmol) and methyl hydrazinecarbimidothioate hydroiodide (0.27 g, 1.16 mmol) were added to the solution. The mixture was stirred for 3hr at room temperature. The reaction mixture was diluted with water (30mL), and extracted with ethyl acetate (3×25 mL). The combined organic layers were washed successively with water (30 mL) and brine (30 mL), dried over sodium sulfate, and concentrated. The crude material was purified by flash chromatography on silica gel, eluted with hexane/ethyl acetate to afford **15** (131 mg, 0.33 mmol, 34 % yield). ^{1}H NMR (400 MHz, DMSO-d_6) δ 10.04 (s, 1H), 9.42 (s, 1H), 7.99 – 7.91 (m, 2H), 7.59 – 7.52 (m, 4H), 7.49 – 7.40 (m, 1H), 2.65 (s, 3H), 2.30 (s, 3H), 1.33 (s, 9H).

[(2-Bromo-6-nitrobenzyl)oxy](*t*-butyl)dimethylsilane (17). To a solution of **16** (9.42 g, 40.6 mmol) in DCM (81 mL) was added imidazole (4.15 g, 60.9 mmol) and *t*-butyldimethylchlorosilane (7.34 g, 48.7 mmol). The mixture was stirred for 4hr at room temperature. The reaction mixture was diluted with water (200 mL), and extracted with DCM (3×50 mL). The combined organic layers were washed successively with water (100 mL), brine (100 mL), and dried over sodium sulfate. The solvent was evaporated to afford **17** (14.5 g, 41.9 mmol, quantitative yield). ^{1}H NMR (400 MHz, Chloroform-*d*) δ 7.73 (ddd, *J* = 8.0, 1.2, 0.5 Hz, 1H), 7.61 (ddd, *J* = 8.0, 1.3, 0.5 Hz, 1H), 7.25 (t, *J* = 8.0 Hz, 1H), 5.03 (s, 2H), 0.86 (s, 9H), 0.06 (s, 6H).

3-Bromo-2-{[(*t*-butyldimethylsilyl)oxy]methyl}aniline (18). To a solution of **17** (14.5 g, 41.9 mmol) in ethanol (291 mL) was added iron (23.38 g, 419 mmol), NH_4Cl (44.8 g, 837 mmol) and water (58.2 ml), and the mixture was stirred for 3hr at 80 °C. The reaction mixture was filtered through a bed of celite to remove insoluble materials. The solvent was concentrated, and the residue was diluted with water (500 mL), and extracted with chloroform (3×300 mL). The combined organic layers were washed successively with water (500 mL), brine (100 mL), dried over sodium sulfate. The solvent was evaporated to afford **18** (12.14 g, 38.4 mmol, 92%). ^{1}H NMR (400 MHz, Chloroform-*d*) δ 6.95 – 6.85 (m, 2H), 6.61 - 6.56 (m, 1H), 4.95 (s, 2H), 4.48 (s, 2H), 0.89 (s, 9H), 0.10 (s, 6H).

***N*-(3-Bromo-2-{[(*t*-butyldimethylsilyl)oxy]methyl}phenyl)-4-(*t*-butyl)benzamide (19)**. Under nitrogen atmosphere, **18** (2.0 g, 6.32 mmol) was dissolved in THF (63 mL) and cooled with an ice bath. To this solution, TEA (1.76 mL, 12.65 mmol) and 4-*t*-butylbenzoyl chloride (1.37 g, 6.96 mmol) were added dropwise, and the mixture was stirred at room temperature for 16 h. The reaction was quenched with water (200 mL), and extracted with ethyl acetate (3×100

mL). The combined organic layers were washed successively with 1N HCl (150 mL), 1 N NaOH (150 mL) and brine (100 mL), then the organic layers were dried over sodium sulfate, and concentrated. The crude material was purified by flash chromatography on silica gel, eluted with hexane/ethyl acetate to afford **19** (2.87 g, 6.02 mmol, 95%). ^{1}H NMR (400 MHz, Chloroform-*d*) δ 9.93 (s, 1H), 8.34 (dd, *J* = 1.18, 8.17 Hz, 1H), 7.95 – 7.80 (m, 2H), 7.50 – 7.44 (m, 2H), 7.31 (dd, *J* = 1.20, 8.08 Hz, 1H), 7.20 (t, *J* = 8.09 Hz, 1H), 5.10 (s, 2H), 1.36 (s, 9H), 0.89 (s, 9H), 0.16 (s, 6H).

4-(*t*-Butyl)-*N*-(2-{[(*t*-butyldimethylsilyl)oxy]methyl}-3-(4,4,5,5-tetramethyl-1,3,2-dioxaborolan-2-yl)phenyl)benzamide (20). To a solution of **19** (3.2 g, 6.72 mmol) in 1,4-dioxane (32 ml) was added bis(pinacolato)diboron (3.41 g, 13.43 mmol), $PdCl_2$(dppf)-CH_2Cl_2 adduct (548 mg, 0.67 mmol) and potassium acetate (1.98 g, 20.15 mmol), and the mixture was stirred for 16hr at 80 °C. The reaction mixture was diluted with water (100 mL) and extracted with ethyl acetate (3×50 mL). The combined organic layers were washed successively with water (100 mL) and brine (100 mL), then the organic layers were dried over sodium sulfate, and concentrated. The crude material was purified by flash chromatography on silica gel, eluted with hexane/ethyl acetate to afford **20** (1.87 g, 3.57 mmol, 53%). ^{1}H NMR (400 MHz, Chloroform-*d*) δ 10.06 (s, 1H), 8.46 (dd, *J* = 1.36, 8.14 Hz, 1H), 7.96 – 7.84 (m, 2H), 7.61 (dd, *J* = 1.38, 7.51 Hz, 1H), 7.53 – 7.42 (m, 2H), 7.36 (t, *J* = 7.78 Hz, 1H), 5.27 (s, 2H), 1.38 – 1.34 (m, 21H), 0.88 (s, 9H), 0.13 (s, 6H).

6-Chloro-N^2-(4-morpholinophenyl)-1,3,5-triazine-2,4-diamine (22). A solution of 4,6-dichloro-1,3,5-triazin-2-amine (124 mg, 0.75 mmol) in THF (1.2 mL) was cooled with an ice bath, and DIEA (0.18 mL, 1.0 mmol) and 4-morpholinoaniline **21** (89 mg, 0.5 mmol) were added to the solution. The mixture was stirred at 0 °C for 1 hr, and then allowed to warm up to room

temperature and the stirring was continued for 16 hr. The resulting solids were collected by filtration, and washed with ethyl acetate to afford **22** as a gray powder (124 mg, 0.40 mmol, 81%). ^{1}H NMR (400 MHz, DMSO-d6) δ9.65 (s, 1H), 7.71 – 7.15 (m, 4H), 6.99 – 6.76 (m, 2H), 3.79 – 3.67 (m, 4H), 3.09 – 2.99 (m, 4H).; LCMS (*m/z*): mass was calculated for $C_{13}H_{15}ClN_6O$ requires 306.1, found 307.1 $[M+H]^+$.

BTK inhibition assay. Recombinant biotinylated human BTK enzymes having a N-terminal DYKDDDDK tag was obtained from Drug Discovery Support Business Division of Carna Biosciences, Inc.

Preparation of activated form of BTK (BTK[A]). A solution of the biotinylated BTK in a buffer solution consisting of 50 mM Tris-HCl (pH 7.5), 150 mM NaCl, 10% Glycerol, 0.05% Brij 35, and 1 mM DTT was treated with 3 mM ATP at 4 °C overnight. The mixture was then run through the 10-DG column to afford BTK [A].

Preparation of unactivated form of BTK (BTK[U]). A solution of the biotinylated BTK in the buffer solution was treated with 10 U/μg of λ protein phosphatase and 2 mM $MnCl_2$ at 4 °C overnight. The mixture was purified by a DYKDDDDK tag antibody agarose gel column, then the buffer was exchanged using the 10-DG column to afford BTK [U].

Measurment of BTK inhibitory activity. Measurement of BTK activity was carried out using MSA assay kit (QuickScout™ Screening Assist Kit, Carna Biosciences, Inc.). Namely, enzymatic activity of BTK[A] and BTK[U] was measured using 1 mM FITC-labeled Srctide peptide in the presence of compounds in assay buffer consisting of 20 mM HEPES (pH 7.5), 0.01% Triton X-100™, 2 mM DTT 5 mM, $MgCl_2$. Then 25 mM ATP or 50 mM ATP was added for biotinylated BTK [A] or biotinylated BTK [U] assays, respectively. The reaction was terminated by adding of EDTA. The quantities of the substrates (S) and the phosphorylated

substrate (P) in the reaction solution were measured using LabChip EZ Reader II system (PerkinElmer, Inc.). The inhibition rate (%) of the test compound was calculated according to the following equation:

$$\textbf{Inhibition rate (\%)} = (1-(C-A)/(B-A)) \times 100$$

A represents P/(P + S) for a blank well, B represents P/(P + S) for a solvent well, and C represents P/(P + S) for a compound-added well. S: the peak heights of the separated substrate, P: phosphorylated substrate.

The IC_{50} value was calculated via a regression analysis of the inhibition rate (%) and the test compound concentration (logarithmic value).

X-ray Crystallography of 2e complexed with BTK. Generation of human BTK protein (residues 393 to 656) for crystallography was conducted as previously reported.[18] Crystallization was carried out using the sitting drop vapor diffusion method. A 1.6 μL of compound **2e** (10 mM DMSO solution) was added to a solution of hBTK (160 μL, 6 mg/mL) and incubated at 4 °C for 16 h prior to set up drops. A drop consisted of 1 μL protein solution and 1 μL reservoir solution containing 0.1 M imidazole (pH7.0), 0.1 M potassium thiocyanate, 30% w/v PEG MME 2000, and 4% v/v polypropylene glycol P 400, and microseeding was performed to initiate crystal growth. The crystals appeared within a few days and continued to grow for 1−2 weeks. Crystals were flash-cooled in liquid nitrogen for data collection with 10% glycerol and 90% reservoir solution as cryoprotectant. Diffraction data were collected by SOSHO, Inc. (Osaka, Japan), Inc. hBTK/compound **2e** cocrystals belonged to the space group *C*2: a = 71.3 Å, b = 41.2 Å, c = 587.9 Å, β = 90.006°. The 2.90 Å resolution structure was determined by molecular replacement using human BTK structure (PDB ID: 3GEN). The structure of hBTK with compound **2e** has been deposited to RCSB with PDB ID: 5ZZ4.

Measurement of BTK inhibition in cells.

Ramos cells (2G6.4C10, ATCC Inc., No. CRL-1923) were cultured in a T75 flask, in a 5% CO_2 incubator, using an RPMI-1640 medium (GIBCO Inc.) containing 10% FBS (AusGene Inc.) and 1% penicillin-streptomycin (Nacalai Inc.). Test compound solution was prepared as 3× concentration of the final concentration, by diluting 10 mM DMSO stock solution with RPMI-1640 medium.

Ramos cells were diluted with RPMI-1640 medium (no serum) to prepare the cell suspension (cell density, 7.5×10^6 cells/mL), and then incubated at 37°C for 45 minutes. 500 μL of the test compound solution was added to 1mL of the cell suspension in a 2.0 mL tube, and incubated at 37°C for 1 hour. Then, anti-IgM Ab (Invitrogen, H15100) was added to the tube (final conc. 10 μg/mL), and incubated at 37°C for 10 minutes. Then the cells were collected as pellets by centrifuge, and 100 μL of lysis buffer [RIPA Buffer (×1) (Cell Signaling Technology, Inc.) containing 1% Phosphatase inhibitor Cacktail 3 (Sigma Co., No. P0044), 1% Phosphatase inhibitor Cacktail (Nacalai Inc., No.07575), and 1 mM phenylmethylsulfonyl fluoride (PMSF) was added, followed by gentle stirring and further standing for 10 minutes. The supernatant was collected by a centrifugal operation at 15,000 rpm for 15 min. The supernatant was mixed with SDS-sample buffer and the mixture was heated at 95°C for 5 minutes. The sample solution (5 μL each) was applied into each well of a 4-20% gradient acrylamide gel (Cosmo Bio Co., Ltd., No. 414879) and then electrophoresis was carried out. The protein in the gel was transferred to a PVDF membrane, using an iBlot gel transfer system (Life Technologies Corporation).

The transferred PVDF membrane was subjected to a blocking treatment with 2% ECL prime blocking Reagent (GE Healthcare Ltd.), and then incubated with a primary antibody at 4°C overnight. The unbound primary antibody was washed with TBST buffer (10 mM Tris-HCl (pH 7.5), 150 mM NaCl, 0.1% Tween 20), and then incubated with a secondary antibody in TBST

buffer containing 2% ECL prime blocking Reagent at room temperature for 1 hour. The unbound secondary antibody was washed with TBST buffer, and treated with ECL Prime Western Blotting Detection System (GE Healthcare Ltd.) according to the attached protocol. Each band was detected by chemiluminescence using a CCD camera (ATTO, Light-CaptureII).

Animal studies. All animal experiments in this study were approved by the Carna Biosciences Animal Care and Use Committee and carried out according to the Carna Biosciences Animal Experimentation Regulation.

Efficacy study of 4b in mouse PCA model. Mice were passively sensitized by intradermal injection of 10 μL anti-DNP IgE in both ears. After 46 hours, diphenhydramine, compound **4b** and vehicle (DMSO:PEG#400:HP-β-CD [30%(w/v)] (5:30:65)) were administered. Then DNP-BSA/dye mixture was administered (0.25 mL/mouse, i.v.) after 10 minutes for diphenhydramine or after 2 hours for compound **4b**. The mice were then sacrificed 30 min after the dye injection, and both ears of each mouse were collected, and weighed. A pair of the ears was dissolved by 1N KOH (0.7 mL) at 37 °C overnight, then 9.3 mL of an acetone/0.6N phosphoric acid (13:5) mixture was added to the suspension, and the mixture was shaken. The extracts were centrifuged (3,000 rpm, 10 min) to remove precipitates, then supernatant was filtered by a 0.2 mm filter. Absorbance at 620 nm was measured to determine the amount of the dye.

Collagen-induced arthritis mouse model. Incomplete Freund's Adjuvant (Chondrex, Inc., #7002) supplemented with M.Tuberculosis H37 Ra, Desiccated (Beckton Dickinson and Company, #231141) at 2.5 mg/mL and Bovine Type II Collagen, 2 mg/mL Solution (Chondrex, Inc., #20022) were mixed in a 1:1 ratio to form an emulsion. DBA/1J mice (10 animals/group) (6-week old, male) were received 0.1 mL of the emulsion by intradermal injection at the base of the tail on Day 0, and the mice were boosted in the same manner on Day 21. The compound in

DMSO:PEG#400:HP-β-CD [30%(w/v)] (5:30:65) was given twice a day orally every day from Day 18 to Day 36 (compound **4b** at 15, 30, or 60 mg/kg). After the boost on Day 21, the development and severity of the arthritis in each extremity was scored visually once in 2 or 3 days by the following scheme: +0 = normal; +1 = swelling and/or redness of paw or one finger; +2 = swelling of 2 or more joints; +3 = swelling of entire paw covering more than two joints; +4 = severe arthritis of paw and entire fingers. The scores of all four extremities were summed up on each mouse basis, and the mean value of 10 animals in each group was represented as an arthritis score (normal "0" up to maximum "16").

ASSOCIATED CONTENT

Supporting Information

The Supporting Information is available free of charge on the ACS Publications website.

Molecular formula strings (CSV)

Synthesis methods of intermediates (**24h-m**, **25** and **26a-i**), Methods for the microsomal stability assay, aqueous solubility assay, hERG assay and kinase selectivity panel assay (PDF)

Accession Codes

PDB code for compound **2e** is 5ZZ4. Authors will release the atomic coordinates and experimental data upon article publication.

AUTHOR INFORMATION

Corresponding Author

* Phone: +81(78)302-7040. E-mail: wataru.kawahata@carnabio.com

Notes

The authors declare no competing financial interest.

ACKNOWLEDGMENT

We would like to thank the scientists at TCG Lifesciences Private Limited for synthetic chemistry support. We acknowledge Dr. Yuko Uno for *in vitro* assay support. We also gratefully acknowledge Carna's Contract Research Department for providing assay kits and performing selectivity profiling.

ABBREVIATIONS

BTK, Bruton's Tyrosine Kinase; CIA, collagen-induced arthritis; PLCγ2, Phospholipase Cγ2; SYK, Spleen tyrosine kinase; Vd, Volume of distribution; MRT, mean residence time; MC, methyl cellulose; DNP, Dinitrophenol; MTX, Methotrexate; DIEA, *N,N*-diisopropylethylamine; EDC, 1-Ethyl-3-(3-dimethylaminopropyl)carbodiimide; HOBt, 1-Hydroxybenzotriazole; TEA, Triethylamine; HP-β-CD, 2-Hydroxypropyl-beta-cyclodextrin.

REFERENCES

1. Satterthwaite, A. B.; Li, Z.; Witte, O. N. Btk function in B cell development and response. *Semin. Immunol*. **1998**, *10*, 309-316.

2. Khan, W. N. Regulation of B lymphocyte development and activation by Bruton's tyrosine kinase. *Immunol Res*. **2001**, *23*, 147-156.

3. Liu, Y.; Zhou, G.; Zhang, B.; Liu, Y. Bruton's tyrosine tinase: structure and functions, expression and mutations. *Gene Technol*. **2013**, *2*, 106.

4. Satterthwaite, A. B.; Witte, O. N. The role of Bruton's tyrosine kinase in B-cell development and function: a genetic perspective. *Immunol. Rev.* **2000**, *175*, 120-127.

5. Kurosaki, T. Functional dissection of BCR signaling pathways. *Curr. Opin. Immunol.* **2000**, *12*, 276-281.

6. Ellmeier, W.; Abramova, A.; Schebesta, A. Tec family kinases: regulation of FceRI-mediated mast-cell activation. *FEBS J*. **2011**, *278*, 1990-2000.

7. Pal Singh, S.; Dammeijer, F.; Hendriks, R. W. Role of Bruton's tyrosine kinase in B cells and malignancies. *Mol. Cancer* **2018**, *17*, 57.

8. Hendriks, R. W.; Yuvaraj, S.; Kil, L. P. Targeting Bruton's tyrosine kinase in B cell malignancies. *Nat. Rev. Cancer.* **2014**, *14*, 219-232.

9. Horwood, N. J.; Urbaniak, A. M.; Danks, L. Tec family kinases in inflammation and disease. *Int. Rev. Immunol*. **2012**, *31*, 87-103.

10. Halcomb, K. E. Btk Regulates Localization, In vivo activation, and class switching of anti-DNA B cells. *Mol. Immunol.* **2008**, *46*, 233-241

11. Davids, M. S.; Brown, J. R. Ibrutinib: a first in class covalent inhibitor of Bruton's tyrosine kinase. *Future Oncol.* **2014**, *10*, 957-967.

12. Wu, J.; Liu, C.; Tsui, S. T.; Liu, D. Second-generation inhibitors of Bruton tyrosine kinase. *J. Hematol. Oncol*. **2016**, *9*, 80-86.

13. Barf, T.; Kaptein, A. Irreversible protein kinase inhibitors: balancing the benefits and risks. *J. Med. Chem*. **2012**, *55*, 6243-6262.

14. Byrd, J. C.; Furman, R. R.; Coutre, S. E.; Burger, J. A.; Blum, K. A.; Coleman, M.; Wierda, W. G.; Jones, J. A.; Zhao, W.; Heerema, N. A.; Johnson, A. J.; Shaw, Y.; Bilotti, E.; Zhou, C.; James, D. F.; O'Brien, S. Three-year follow-up of treatment-naive and previously treated patients with CLL and SLL receiving single-agent Ibrutinib. *Blood* **2015**, *125*, 2497-506.

15. Byrd, J. C.; Furman, R. R.; Coutre, S. E.; Flinn, I. W.; Burger, J. A.; Blum, K. A.; Grant, B.; Sharman, J. P.; Coleman, M.; Wierda, W. G.; Jones, J. A.; Zhao, W.; Heerema, N. A.; Johnson, A. J.; Sukbuntherng, J.; Chang, B. Y.; Clow, F.; Hedrick, E.; Buggy, J. J.; James, D. F.; O'Brien, S. Targeting BTK with Ibrutinib in relapsed chronic lymphocytic leukemia. *New Engl. J. Med*. **2013,** *369*, 32-42.

16. Berglöf, A.; Hamasy, A.; Meinke, S.; Palma, M.; Krstic, A.; Månsson, R.; Kimby, E.; Österborg, A.; Smith, C. I. Targets for Ibrutinib beyond B cell malignancies. *Scand. J. Immunol*. **2015**, *82*, 208-17.

17. Liang, C.; Tian, D.; Ren, X.; Ding, S.; Jia, M.; Xin, M.; Thareja, S. The development of Bruton's tyrosine kinase (BTK) inhibitors from 2012 to 2017: A mini-review. *Eur. J. Med. Chem*. **2018**, *151*, 315-326.

18. Kawahata, W.; Asami, T.; Irie, T.; Sawa, M. Design and synthesis of novel pyrimidine analogs as highly selective, non-covalent BTK inhibitors. *Bioorg. Med. Chem. Lett*. **2018**, *28*, 145-151.

19. Asami, T.; Kawahata, W.; Sawa, M. TR-FRET binding assay targeting unactivated form of Bruton's tyrosine kinase. *Bioorg. Med. Chem. Lett*. **2015**, *25*, 2033-2036.

20. Kawahata, W.; Asami, T.; Fujii, I.; Sawa, M. 'Turn On/Off' fluorescence probe for the screening of unactivated Bruton's tyrosine kinase. *Bioorg. Med. Chem. Lett*. **2015**, *25*, 2141-2145.

21. Di Paolo, J. A.; Huang, T.; Balazs, M.; Barbosa, J.; Barck, K. H.; Bravo, B. J.; Carano, R. A. D.; Darrow, J.; Davies, D. R.; DeForge, L. E.; Diehl, L.; Ferrando, R.; Gallion, S. L.; Giannetti, A. M.; Gribling, P.; Hurez, V.; Hymowitz, S. G.; Jones, R.; Kropf, J. E.; Lee, W. P.; Maciejewski, P. M.; Mitchell, S. A.; Rong, H.; Staker, B. L.; Whitney, J. A.; Yeh, S.; Young, W. B.; Yu, C.; Zhang, J.; Reif, K.; Currie, K. S. Specific Btk inhibition suppresses B cell- and myeloid cell-mediated arthritis. *Nat. Chem. Biol*. **2011**, *7*, 41-50.

22 Lou, Y.; Han, X.; Kuglstatter, A.; Kondru, R. K.; Sweeney, Z. K.; Soth, M.; McIntosh, J.; Litman, R.; Suh, J.; Kocer, B.; Davis, D.; Park, J.; Frauchiger, S.; Dewdney, N.; Zecic, H.; Taygerly, J. P.; Sarma, K.; Hong, J.; Hill, R. J.; Gabriel, T.; Goldstein, D. M.; Owens, T. D. Structure-based drug design of RN486, a potent and selective Bruton's tyrosine kinase (BTK) inhibitor, for the treatment of rheumatoid arthritis. *J. Med. Chem*. **2015**, *58*, 512–516.

23. Chang, B. Y.; Huang, M. M.; Francesco, M.; Chen, J.; Sokolove, J.; Magadala, P.; Robinson, W. H.; Buggy, J. J. The Bruton tyrosine kinase inhibitor PCI-32765 ameliorates autoimmune arthritis by inhibition of multiple effector cells. *Arthritis Res. Ther.* **2011**, *13*, R115.

24. Hajbi, Y.; Suzenet, F.; Khouili, M.; Lazar, S.; Guillaumet, G. Polysubstituted 2,3-dihydrofuro[2,3-*b*]pyridines and 3,4-dihydro-*2H*-pyrano[2,3-*b*]pyridines via microwave-activated Inverse electron demand Diels-Alder reactions. *Tetrahedron* **2007**, *63*, 8286-8297

25. Pellegatti, L.; Vedrenne, E.; Leger, J. M.; Jarry, C.; Routier, S. New heteroaromatic aminations on 5-aryl-1,2,4-triazines and 1,2,4,5-tetrazines by palladium catalysis. *Tetrahedron* **2010**, *66*, 4383-4389.

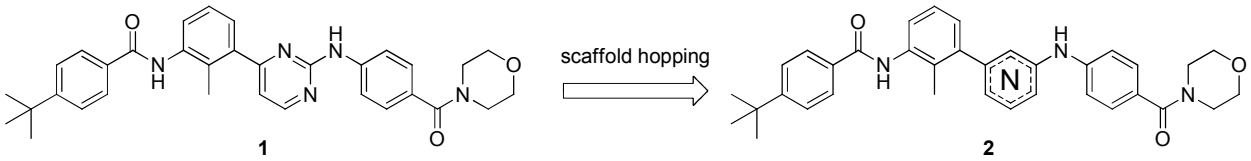

Figure 1. Scaffold hopping of core structure.

Table 1. Initial SAR study for the core structure and its substituents.

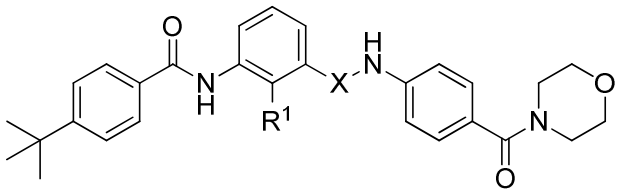

Compound	X	R^1	IC_{50} (nM) [a]	
			BTK[A]	BTK[U]
1	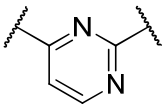	Me	1800	2.3
2a	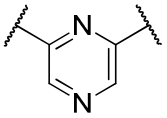	Me	2500	100
2b	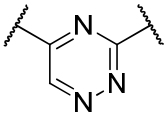	Me	5600	10
2c	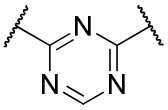	Me	1800	6.4
2d	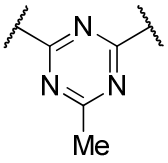	Me	7800	34
2e	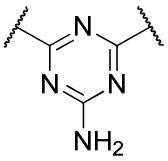	Me	190	0.67

2f	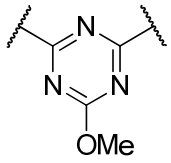	Me	>10000	80
2g	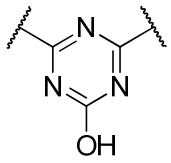	Me	>10000	8800
2h	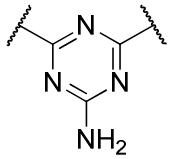	CH_2OH	43	<0.3

[a] Values are the mean of two separate experiments. See Experimental Section for the assay details. All values are rounded to two significant digits.

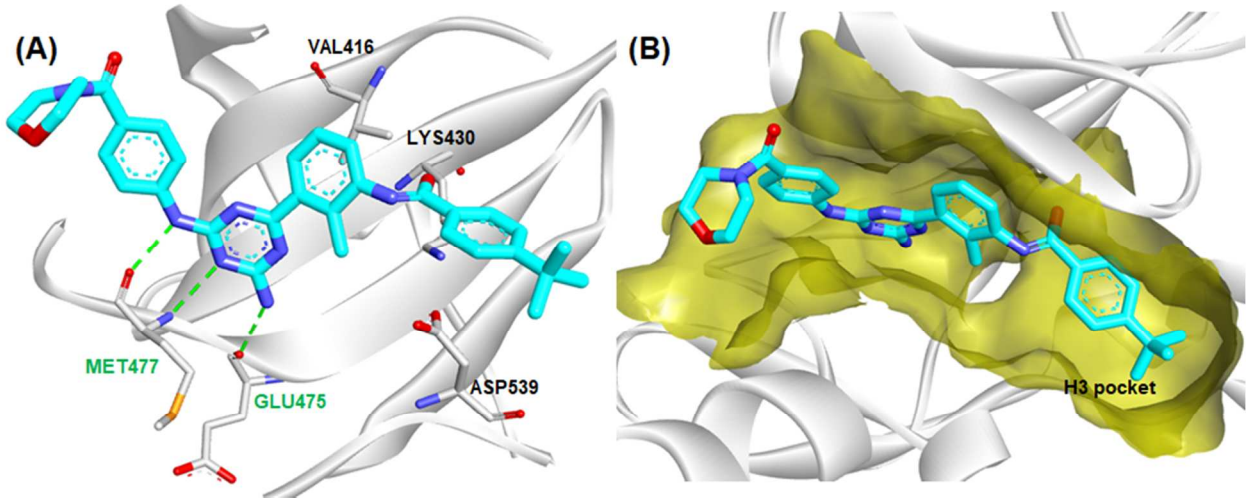

Figure 2. X-ray co-crystal structure of BTK complexed with **2e** (PDB 5ZZ4). (A) Key interactions of **2e** in the BTK active site. Hydrogen bonds are shown as green dotted lines. (B) Surface presentation on binding of **2e** to BTK.

Table 2. Exploration of H3 pocket binder with simple amide

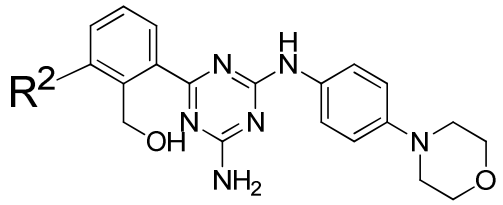

Compound	R^2	IC_{50} (nM) [a]		Metabolic stability [b] (% remain @ 30min)	
		BTK[A]	BTK[U]	human	mouse
3a	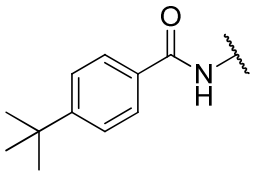	43	0.74	2.9	19
3b	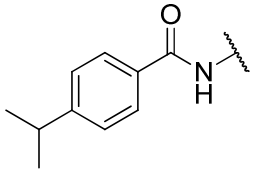	82	2.5	NT	NT
3c	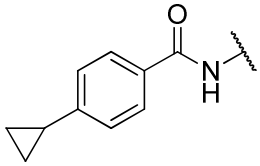	140	2.1	42	1.1
3d	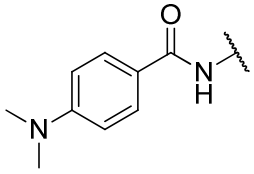	38	4.7	39	52
3e	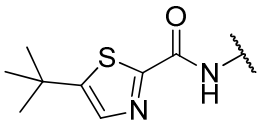	2500	15	NT	NT

3f	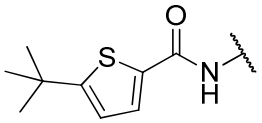	820	4.0	NT	NT
3g	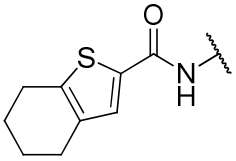	28	0.81	1.7	0.14

[a] Values are the mean of two separate experiments. [b] Remaining % of parent compounds after 30 min treatment of liver microsomes. See Supporting Information for assay details. NT : not tested. All values are rounded to two significant digits.

Table 3. Exploration of H3 pocket binder with cyclic amide analogs.

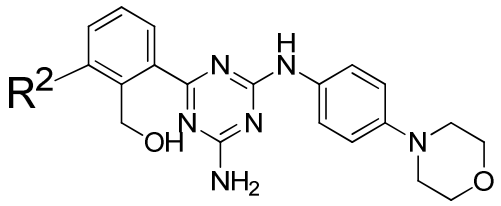

Compound	R^2	IC_{50} (nM) [a]		Metabolic stability [b] (% remain @ 30min)	
		BTK[A]	BTK[U]	human	mouse
3h	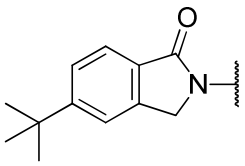	640	3.8	NT	NT
3i	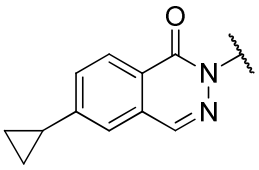	280	4.3	69	75
3j	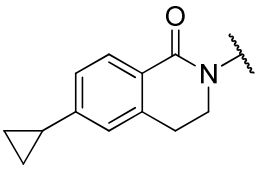	350	4.2	NT	NT
3k	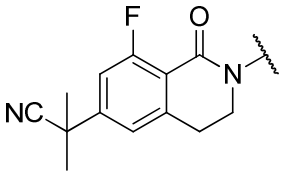	110	1.6	60	59

3l	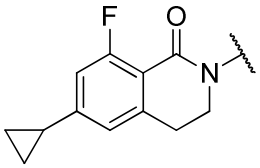	70	2.2	69	6.0
3m	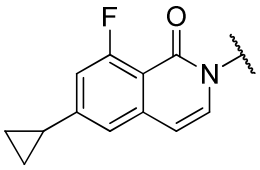	17	0.41	50	13
3n	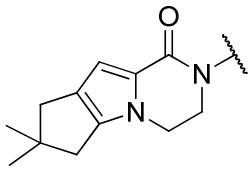	42	0.62	1.39	NT

[a] Values are the mean of two separate experiments. [b] Remaining % of parent compounds after 30 min treatment of liver microsomes. See Supporting Information for assay details. NT : not tested. All values are rounded to two significant digits.

Table 4. SAR study of pyrazole and cyanopyrrole analogs.

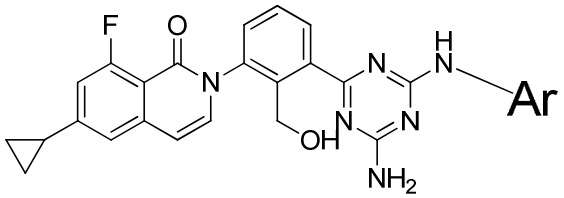

Compound	Ar	IC_{50} (nM) [a]		Metabolic stability [b] (% remain @ 30min)		Aqueous solubility [c] (μM)	hERG inhibition IC_{50} (μM) [d]
		BTK[A]	BTK[U]	human	mouse		
3m	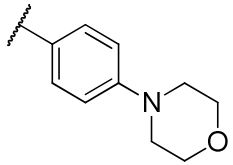	17	0.41	50	13	1.2	NT
4a	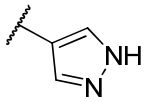	9.3	0.51	100	39	12	NT
4b	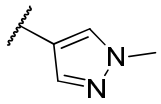	4.2	0.39	83	66	20	24
4c	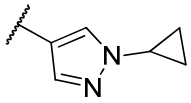	8.3	0.57	79	16	4.7	9.5

4d	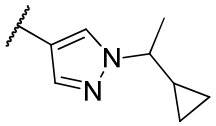	2.2	0.49	51	1.1	2.0	13.5
4e	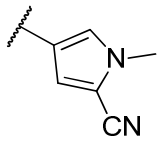	7.4	0.39	66	46	0.67	2.6
4f	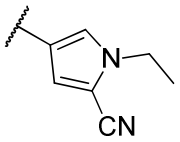	6.3	0.58	59	32	0.71	7.8
4g	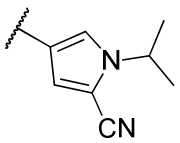	5.4	0.53	47	19	4.8	>30
4h	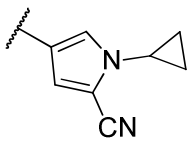	9.1	0.86	69	21	4.0	>30
4i	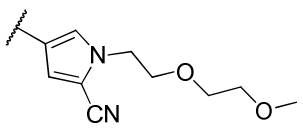	5.1	0.54	4.0	4.7	9.5	NT

[a] Values are the mean of two separate experiments. [b] Remaining % of parent compounds after 30 min treatment of liver microsomes. [c] Solubility values of compounds were determined by kinetic solubility measurement method. [d] IC_{50} values of hERG inhibition were determined by patch-clamp method. See Supporting Information for assay details. NT : not tested. All values are rounded to two significant digits.

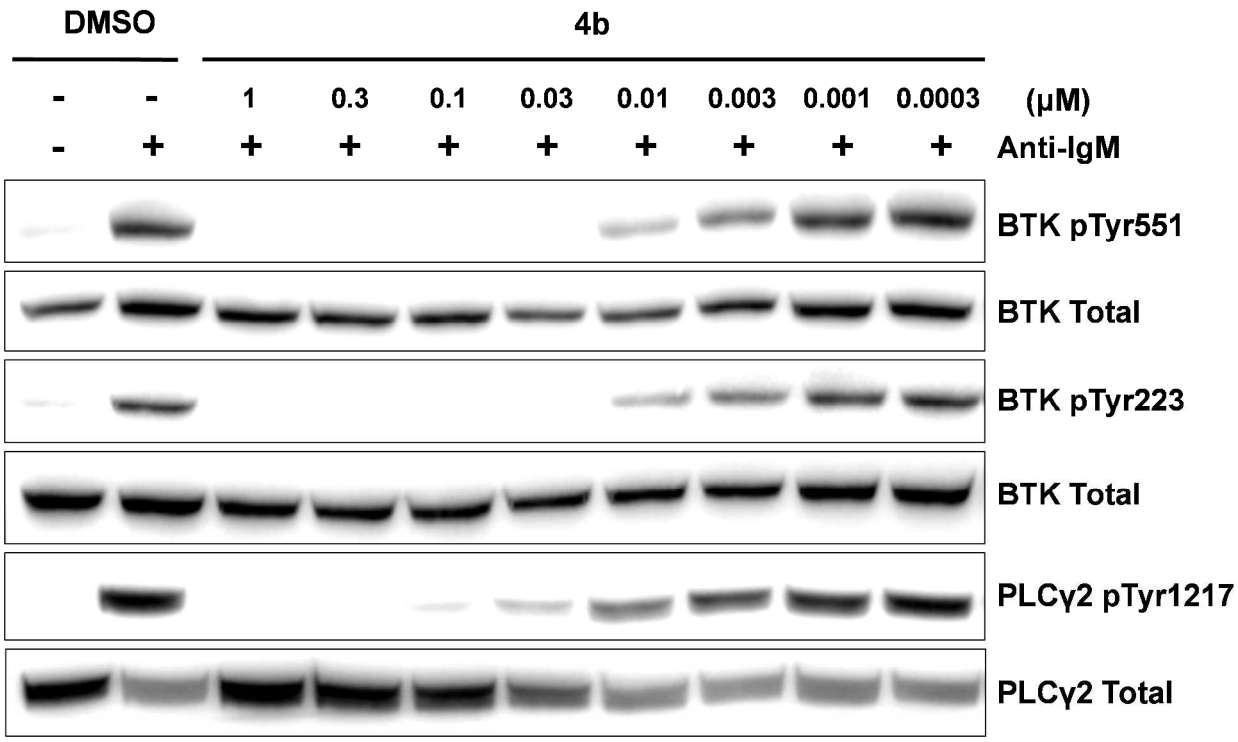

Figure 3. Inhibition of anti-IgM-stimulated phosphorylation of BTK and PLCγ2 in Ramos cells. Ramos cells were treated with **4b** at various concentrations for 1 h and then stimulated with anti-IgM for 10 min. The phosphorylation levels of BTK (Tyr223, Tyr551) and PLCγ2 (Tyr1217) were analyzed by western blotting.

Table 5. Pharmacokinetic parameters of **4b** [a].

Species	Dosage and route	$t_{1/2}$ hr	T_{max} hr	C_{max} ng/mL	$AUC_{(0-t)}$ ng/mL*hr	$AUC_{(0-\infty)}$ ng/mL*hr	Vd L/kg	Cl L/hr/kg	$MRT_{(0-\infty)}$ hr	F %
Mice	IV-2 mg/kg [b]	3.27	-	2887	3107	3114	3.03	0.64	1.30	-
	PO-10 mg/kg [b]	0.95	0.50	4619	10208	10242	-	-	1.56	65. 8
Rats	IV-1 mg/kg [b]	1.51	-	1376	1917	1960	1.10	0.51	1.79	-
	PO-10 mg/kg [b]	2.44	2.00	1476	8696	8706	-	-	4.88	44.4
Dogs	IV-1 mg/kg [c]	3.91	-	4963	11321	11479	0.29	0.088	3.31	
	PO-2 mg/kg [d]	3.59	2.00	2090	9851	10032	-	-	-	43.7

[a] Values are the mean of three animals. [b] Free base, Vehicle: 5% DMSO/30% PEG400/65% (30% w/v HP-β-CD in water). [c] Sulfate salt, Vehicle: 5% DMSO/5% Solutol HS 15/90% Saline. [d] Sulfate salt, Vehicle: 0.5% MC.

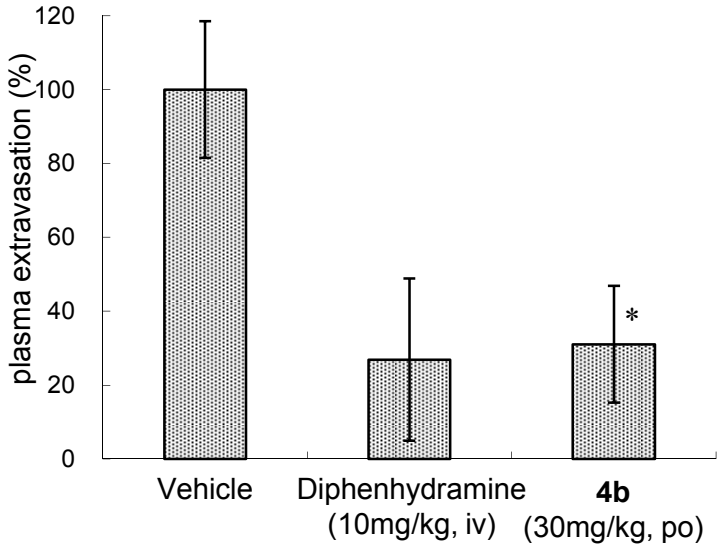

Figure 4. Efficacy of **4b** in mouse PCA model. See Experimental Section for the experimental details. Dunnett's test :* $p < 0.05$

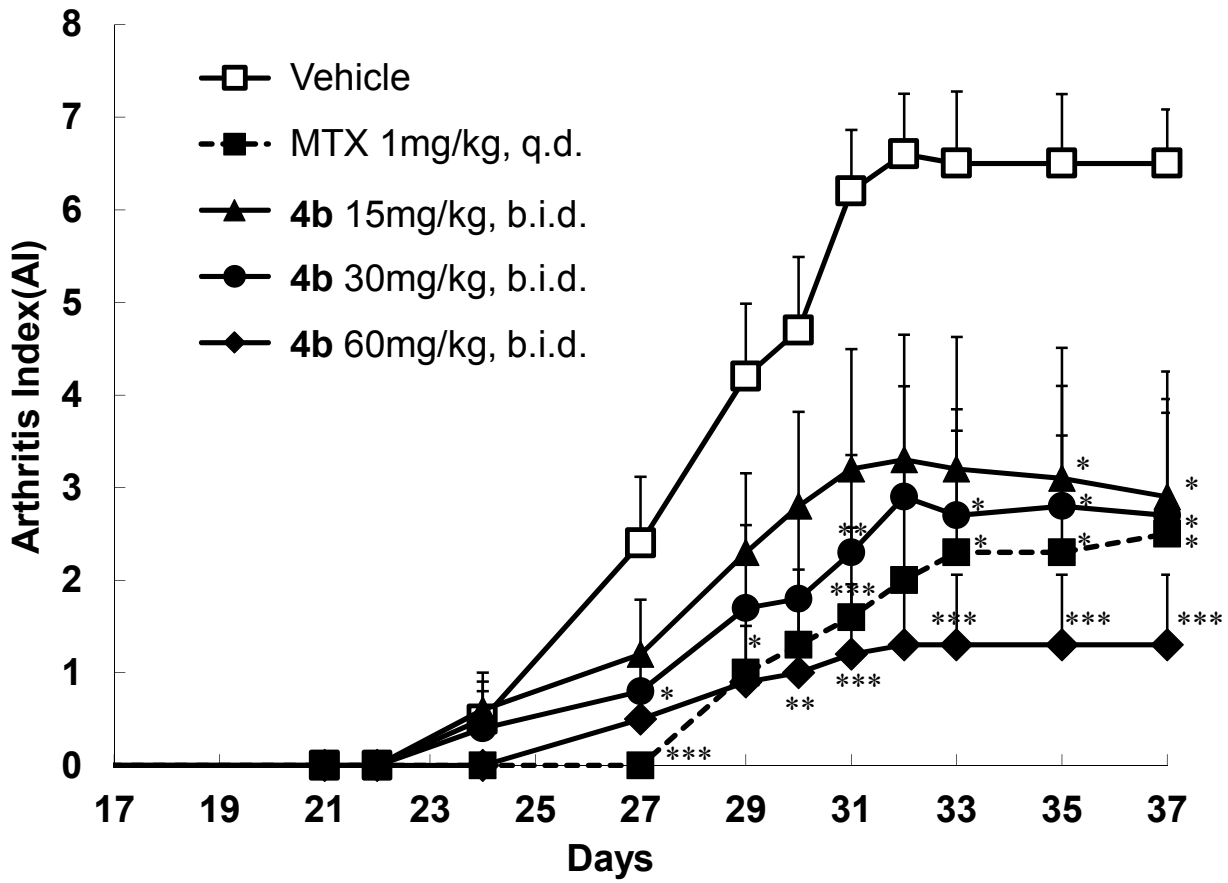

Figure 5. Efficacy of **4b** in collagen-induced arthritis (CIA) mouse model. See Experimental Section for the experimental details. Dunnett's test : *P<0.05, **P<0.01, ***P<0.001

Scheme 1. Synthesis of **2a - 2h**[a]

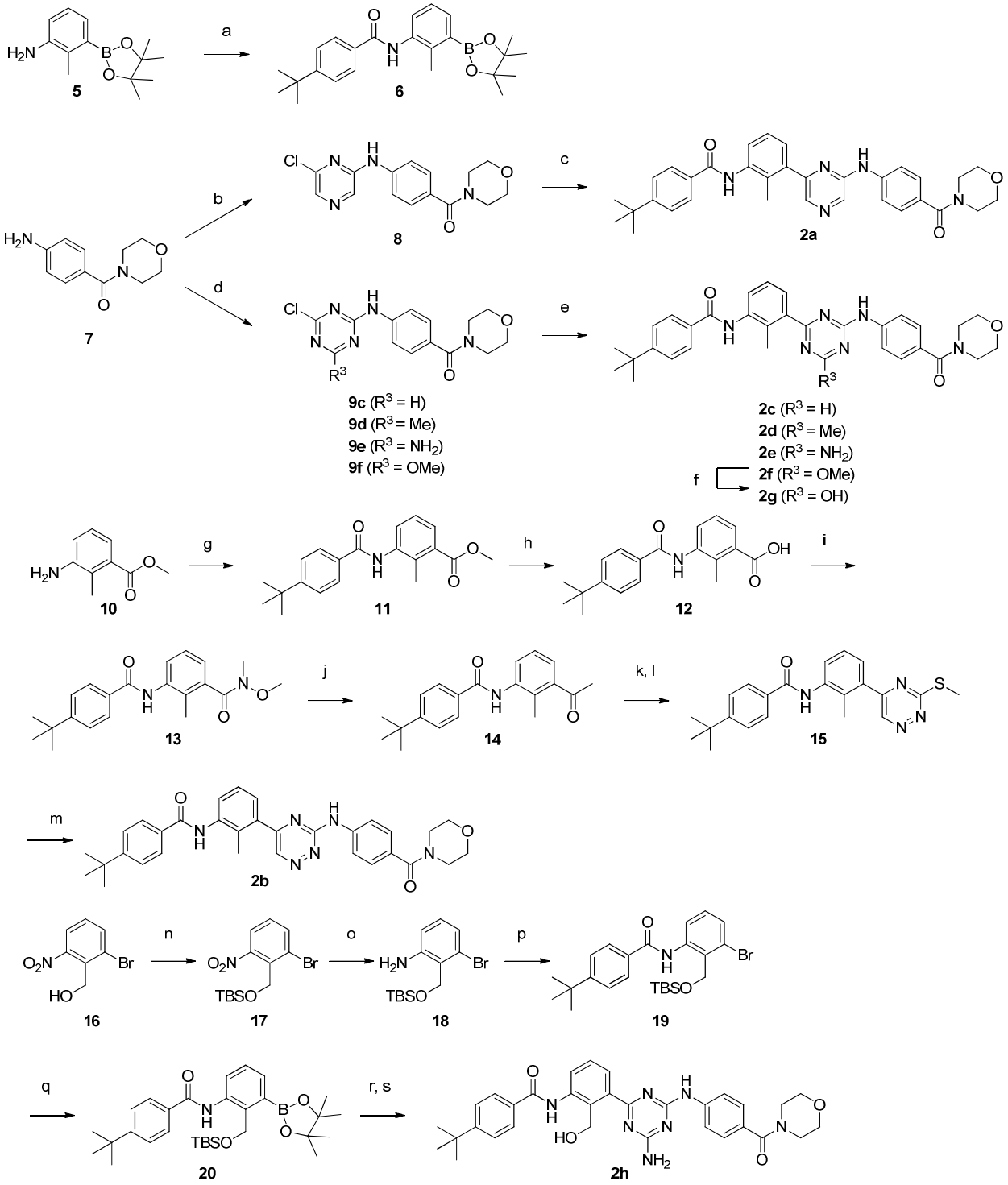

[a] Reagents and conditions: (a) 4-*t*-butylbenzoyl chloride, pyridine, DCM, rt; (b) 2,6-dichloropyrazine, $Pd_2(dba)_3$, sodium *t*-butoxide, 90 °C; (c) **6**, $Pd(PPh_3)_4$, $NaHCO_3$, DME, water,

110 °C; (d) dichloro-1,3,5-triazines (non-substituted, 6-methyl, or 2-amino), DIEA, DMF, 0 °C or 2,4-dichloro-6-methoxy-1,3,5-triazine, DIEA, MeOH, 0 °C; (e) **6**, $Pd(PPh_3)_4$, K_2CO_3, DME, water, 110 °C; (f) 4 M HCl in dioxane, MeOH, 50 °C; (g) 4-*t*-butylbenzoyl chloride, TEA, DCM, rt; (h) 1 M-NaOHaq., THF, MeOH, rt; (i) *N,O*-dimethylhydroxylamine hydrochloride, EDC, HOBt, TEA, DMF, rt; (j) methylmagnesium bromide, THF, 0 °C - rt; (k) selenium oxide, 1,4-dioxane, water, 100 °C; (l) *S*-methylisothiosemicarbazide hydroiodide, Na_2CO_3, ethanol, rt; (m) **7**, copper(I) 3-methylsalicylate, cesium carbonate, palladium(II) acetate, xantphos, toluene, 180 °C; (n) TBSCl, imidazole, DCM, rt; (o) Fe, NH_4Cl, 80 °C; (p) 4-*t*-butylbenzoyl chloride, TEA, THF, rt; (q) bis(pinacolato)diboron, $Pd(dppf)Cl_2$-CH_2Cl_2, potassium acetate, 1, 4-dioxane, 80 °C; (r) **9e**, $Pd(PPh_3)_4$, K_2CO_3, DME, water, 110 °C; (s) 1 M TBAF in THF, THF, rt.

Scheme 2. Synthesis of **3a - 3n**[a]

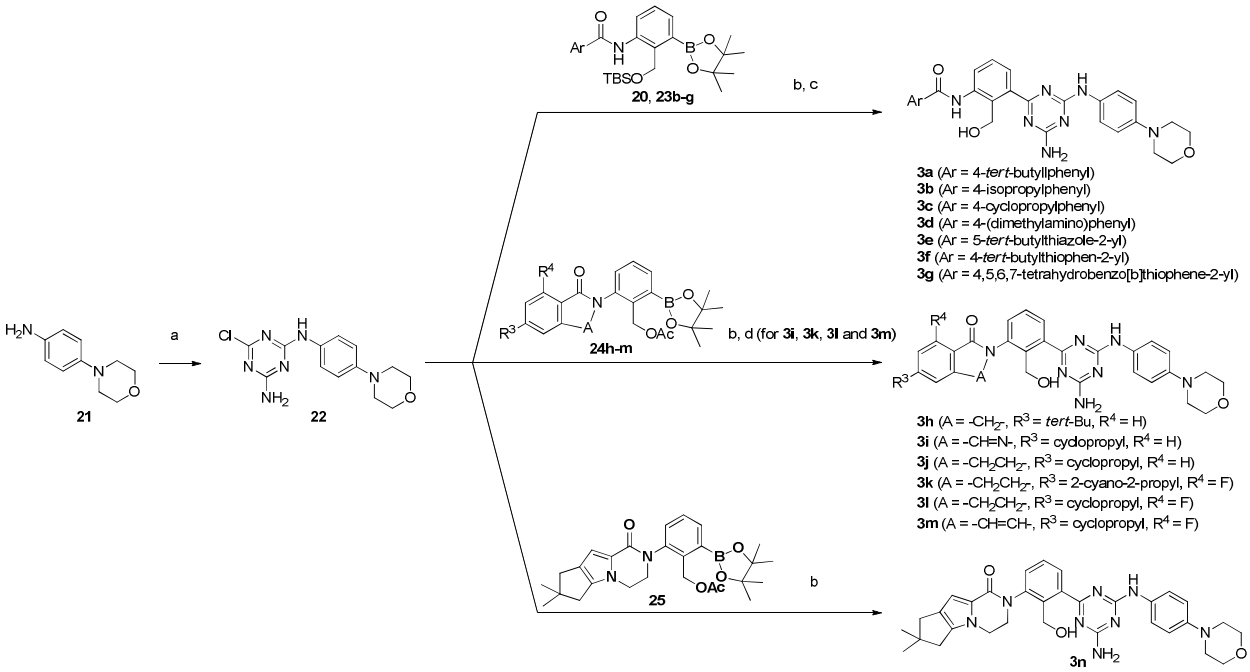

[a] Reagents and conditions: (a) 2-amino-4,6-dichloro-1,3,5-triazine, DIEA, THF, 0 °C; (b) $Pd(PPh_3)_4$, K_2CO_3, DME, water, 110 °C; (c) 1 M TBAF in THF, THF, rt; (d) K_2CO_3, MeOH, THF, rt - 60 °C.

Scheme 3. Synthesis of **4a - 4i**[a]

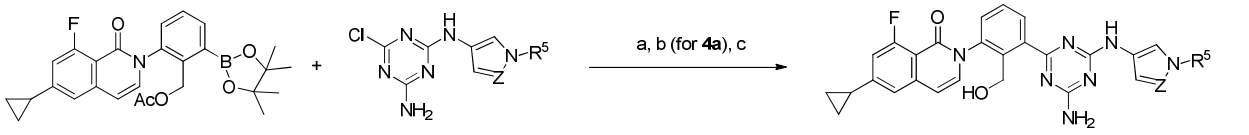

26a (Z = N, R^5 = tetrahydropyranyl)
26b (Z = N, R^5 = methyl)
26c (Z = N, R^5 = cyclopropyl)
26d (Z = N, R^5 = cyclopropylethyl)
26e (Z = C-CN, R^5 = methyl)
26f (Z = C-CN, R^5 = ethyl)
26g (Z = C-CN, R^5 = isopropyl)
26h (Z = C-CN, R^5 = cycloprolyl)
26i (Z = C-CN, R^5 = 2-(2-methoxyethoxy)ethyl)

4a (Z = N, R^5 = H)
4b (Z = N, R^5 = methyl)
4c (Z = N, R^5 = cyclopropyl)
4d (Z = N, R^5 = cyclopropylethyl)
4e (Z = C-CN, R^5 = methyl)
4f (Z = C-CN, R^5 = ethyl)
4g (Z = C-CN, R^5 = isopropyl)
4h (Z = C-CN, R^5 = cycloprolyl)
4i (Z = C-CN, R^5 = 2-(2-methoxyethoxy)ethyl)

[a] Reagents and conditions: (a) $Pd(PPh_3)_4$, K_2CO_3, DME, water, 110 °C; (b) TsOH, MeOH, 60 °C; (c) K_2CO_3, MeOH, rt - 60 °C.

Table of contents graphic